



Uncovering the Impact of Urban Functional Zones on Air Quality in China

Lulu Yuan^{1, #}, Wenchao Han^{2, #,*}, Jiachen Meng³, Yang Wang^{1,*}, Haojie Yu¹, Wenze Li²

¹College of Earth and Environmental Sciences and College of Atmospheric Sciences, Lanzhou University, Lanzhou, China

⁵ ²State Key Laboratory of Environmental Criteria and Risk Assessment, Chinese Research Academy of Environmental Sciences, Beijing, China

³Emergency Management College, Nanjing University of Information Science & Technology, Nanjing, China

#These authors contributed equally to this work.

*Correspondence to: Wenchao Han (han.wenchao@craes.org.cn) and Yang Wang (wang_yang@lzu.edu.cn)

10 **Abstract.** This study presents a comprehensive spatiotemporal analysis of air quality across various urban functional zones in China from 2017 to 2022, uncovering distinct impacts on air quality due to the unique characteristics of each zone. A general decrease in various pollutant concentrations is observed, a result of stringent pollution control policies. Residential, commercial, and industrial zones show significant declines, whereas the transportation zone experiences the least decrease. However, ozone levels rebound significantly in densely populated residential and commercial zones, and exhibit distinct weekend effects. The
15 research highlights U-shaped seasonal patterns for five key pollutants and inverse seasonal patterns for ozone, which gradually decrease. Furthermore, the daily and seasonal variations of pollutant concentrations in industrial zone are the largest, while those in the public management and service zone are the smallest. Notably, spatial heterogeneity is evident, with regional pollutant distributions linked to local emissions, control measures, urban morphology, and climate variability. These findings indicate that, in the future, the Chinese government should curb ozone pollution, strengthen air pollution control in
20 transportation zone, and formulate more scientific and accurate air pollution control policies based on the local situation of each city. This study emphasizes the critical link between urbanization and air quality, advocating for continuous monitoring and the development of zone-specific air quality strategies to ensure sustainable urban environments.

1 Introduction

The rapid development of the world economy and the ongoing trend of urbanization have made air pollution an inescapable
25 environmental issue, with effectively managing and reducing it becoming a hotly debated topic across all social classes (Li et al., 2023; Wen et al., 2024; Zhang et al., 2022c). Over long periods, air pollutants interact with radiation, clouds, and water vapor, thereby altering global and regional climates (Fan et al., 2013; Li et al., 2017). Additionally, air pollution triggers a variety of short-term extreme weather events, such as extreme precipitation, floods, droughts, wildfires, and heat waves (He et al., 2024; Rosenfeld et al., 2008). Numerous studies have demonstrated the close association of air pollution with
30 neurological diseases, cardiovascular diseases, and lung cancer, significantly impacting human health (Berg et al., 2023; Qin et al., 2023; Ward-Caviness and Cascio, 2023). The frequent changes in urban land use and the increased intensity of land use due to urbanization will lead to significant changes in the emissions and dispersion conditions of urban air pollutants, altering the spatial distribution of air pollution within cities (Qi et al., 2022; Qian et al., 2022). Consequently, it is crucial to study how urban underlying surfaces influence the spatial distribution of air pollutants to enhance our understanding of the interaction
35 between urbanization and air pollution, as well as to improve the accuracy of air pollution control measures.

Situated in Eastern Asia with an expansive landmass spanning 9.6 million square kilometers characterized by diverse topography and notable regional climatic variations (Chen and Sun, 2015; Wang, 2010), China stands as both the world's largest developing nation and leading emitter boasting a substantial agricultural economy and population base (Chen and Gong, 2021). Since 2013, rigorous national pollution standards along with strategic control initiatives like "the Air Pollution



40 Prevention and Control Action Plan" (SC, 2013) and "the Three-Year Action Plan for Winning the Blue Sky Defense Battle" (SC, 2018) have significantly enhanced air quality; however, levels of PM₁₀, PM_{2.5}, and O₃ persist well above World Health Organization benchmarks (Liu et al., 2023; Zeng et al., 2019).

45 Based on data from remote sensing and station observations, the majority of previous research has examined the regional and temporal distribution of air pollution in China across various spatial and temporal scales. In terms of temporal scale, numerous studies have analyzed the changing trends of various pollutants in recent years based on inter-annual variations. The findings indicate that the concentration of O₃ has been the only one to increase, while the concentrations of other pollutants (PM_{2.5}, PM₁₀, SO₂, NO₂, and CO) have decreased year by year (Deng et al., 2022; Fan et al., 2020; Yang et al., 2024). From the perspective of seasonal variation, the concentrations of PM_{2.5}, PM₁₀, SO₂, NO₂, and CO exhibit a U-shaped distribution, characterized by higher concentrations in winter and lower concentrations in summer; conversely, O₃ demonstrates a 50 distribution that is inversely U-shaped (Dong et al., 2022; Fang et al., 2022; Wang et al., 2022c). Regarding diurnal variation, the diurnal concentration of PM_{2.5} displays a bimodal trend, whereas SO₂ and O₃ exhibit unimodal patterns (Liu et al., 2024; Qin et al., 2021; Zhao et al., 2016). In terms of spatial scale, the concentration of pollutants other than O₃ reaches the highest value in North China across different regions (Fan et al., 2020; Kuerban et al., 2020). When considering different provinces, the high concentration areas of particulate matter (PM_{2.5} and PM₁₀) are mainly found in Hebei, Henan, Shandong, and Xinjiang 55 provinces; the SO₂ concentration is highest in Shanxi Province, the lowest in Hainan Province, and the high concentration area of CO is also in Shanxi Province (Wang et al., 2022c; Zhao et al., 2021a). From the perspective of different urban agglomerations, the PM_{2.5} concentration in the Beijing-Tianjin-Hebei urban agglomeration has decreased the most in recent years, and the high concentration area of air pollutants has gradually shifted southward to the Central Plains urban agglomerations, and it is observed that pollutant concentration significantly correlates with the level of economic development 60 and population density (Qi et al., 2023; Tao et al., 2022).

There exists a significant correlation between urbanization and air pollution. Airborne pollutants have the ability to disperse and absorb solar radiation, leading to a reduction in ground-level solar radiation intensity (Fan et al., 2018b; Zhang et al., 2022b). On the other hand, air pollutants can affect the relative humidity of clouds, leading to changes in cloud thickness and coverage, and the radiation from clouds also changes accordingly, which in turn affects the rainfall and thunderstorms in urban 65 areas (Guo et al., 2016; Wilcox et al., 2016). Furthermore, air pollutants can also alter the intensity of urban heat islands by changing the atmospheric temperature above the city, altering the stability of the boundary layer and vertical movements, as well as reducing diurnal temperature fluctuations (Cao et al., 2016; Han et al., 2020; Youn et al., 2023).

Changes in anthropogenic emissions and the spatial structure of urban underlying surfaces caused by urbanization will have an important impact on the formation, transmission, and distribution of air pollutants in urban areas (Ban et al., 2023; Shen et 70 al., 2017; Yang et al., 2020). Pollutant discharge has a direct impact on the concentration levels and spatial distribution of pollutants in the atmosphere (Li et al., 2022c; Zawacki et al., 2018). Changes in the spatial structure of urban underlying surfaces not only change the spatial pattern of pollutant emissions but also affect the diffusion conditions of pollutants through changes in urban heat island effect (UHI) and urban canopy meteorological forcing (UCMF), affecting the spatial distribution 75 of air pollutants (Fan et al., 2018a; Huszar et al., 2022; Zhong et al., 2018). Based on urban land use data and built-up area data, many studies have characterized the spatial structure of the underlying urban surfaces through parameters such as urban compactness index and landscape pattern index, and have found that urban form and urban scale affect the distribution and diffusion of air pollutants, especially in PM_{2.5}, NO₂, and O₃ (Chen and Wei, 2024; Huang et al., 2021a; Liu et al., 2022; Tao et al., 2020; Zhang et al., 2022a). Some studies have found that the impact of urban landscape form on air quality varies according 80 to city size and location, and generally small-scale, decentralized, and multi-center cities have better air quality (Li and Zhou, 2019; Mao et al., 2022; Zhao et al., 2022; Zhu et al., 2023). The influence of urban landscape patterns on pollutant concentrations has also shown significant spatial heterogeneity. Patch density (PD) in Henan and Shandong provinces showed a significant positive correlation with PM_{2.5} concentrations, while the urban PD in Northeast China showed a significant



negative correlation with $PM_{2.5}$ concentrations. The correlation between landscape patterns and $PM_{2.5}$ concentrations in inland and coastal cities is also significantly different. The landscape in the built-up area of Hohhot has a significant positive effect
85 on $PM_{2.5}$ concentrations, and the landscape in green space has a significant inhibitory effect on $PM_{2.5}$ concentrations, but this effect is not as obvious in Tianjin. The correlation between landscape patterns and $PM_{2.5}$ concentrations also varies within different areas of the same city. The density of industrial buildings in suburban Shenzhen is significantly positively correlated with $PM_{2.5}$ concentrations, while in downtown Shenzhen it is negatively correlated (Duan et al., 2021; Shen et al., 2023; Wang et al., 2019). In addition, the influence of urban landscape patterns on $PM_{2.5}$ concentrations also has seasonal and scale effects,
90 which is significant in summer at the regional scale and even more so in winter at the urban grid scale (Li et al., 2021; Meng et al., 2023).

Although numerous studies have been conducted on the relationship between urbanization and air pollution, no relevant research has been found regarding the impact of urban functional zones on air quality. The significant differences in emissions between various urban functional zones, such as residential, industrial, and transportation areas, coupled with the distinct types
95 of spatial structures of underlying surfaces, lead to divergent impacts on the evolution of atmospheric pollutants across these zones. Nevertheless, the specific influence of various urban functional zones on air pollution dynamics remains unclear. A comprehensive analysis of the spatio-temporal evolution of urban air quality in China from the perspective of urban functional zones can offer novel insights and methodologies for preventing and controlling urban air pollution, as well as guiding future urban planning and environmental management practices.

100 Therefore, drawing upon extensive ground station observation data spanning several years, this study aims to conduct a systematic and comprehensive analysis of the spatio-temporal evolution characteristics of air pollutants across various functional zones within Chinese urban areas from 2017 to 2022. This analysis will encompass multiple temporal scales (yearly, seasonal, weekly, daily) as well as diverse spatial dimensions (geographical regions and urban agglomerations), while also examining their potential influencing factors. The specific research design is as follows: the second chapter is the data and
105 methods, the third chapter is the results and discussion, and the fourth chapter is the conclusion.

2 Data and methods

2.1 Study area

China is located in the eastern part of Asia, on the western coast of the Pacific Ocean, with a large span of latitudes. It has a vast territory and a terrain that is undulating and varied, which can be roughly divided into three levels of steps, with the
110 altitude gradually decreasing from west to east. The complex and diverse topography has led to a complex and diverse range of climate types (Cheng et al., 2018; Liu and Liu, 2023). The climates in China include tropical monsoon climate, subtropical monsoon climate, temperate monsoon climate, temperate continental climate, and plateau mountain climate. As the globe's foremost consumer of resources and the second-largest economy, China has witnessed remarkable economic expansion over recent decades, propelled by its abundant human capital and ongoing industrialization processes (Dmitrienko et al., 2023; Guo et al., 2013; Zhang et al., 2023). This study divides China into six major regions based on geographical characteristics and administrative divisions: North China, Northeast China, East China, Central South, Southwest, and Northwest.

In 2018, the Chinese government launched the Three-Year Action Plan for Winning the Blue Sky Defense Battle, which identified three key areas for air pollution control: the Beijing-Tianjin-Hebei region and its surrounding areas, the Yangtze River Delta region, and the Fen-Wei Plain. The Beijing-Tianjin-Hebei region and its surrounding areas include 28 cities, such
120 as Beijing; the Yangtze River Delta region includes 41 cities, such as Shanghai; the Fen-Wei Plain includes 11 cities, such as Xi'an.

In this study, 336 prefecture-level cities in China are selected as research objects, which have great differences in natural conditions, economic development, and industrial structure. As the scale of Chinese cities continues to expand and the



economic strength of cities continues to increase, the Chinese government promulgated the National New Urbanization Plan
125 (2014–2020) in 2014, which proposed a "5-8-6" pattern of urban agglomerations, namely 5 national urban agglomerations, 8
regional urban agglomerations, and 6 local urban agglomerations. The 14th Five-Year Plan further emphasizes the promotion
of 19 urban agglomerations (He et al., 2022; Ouyang et al., 2021). This study will focus on six major urban agglomerations
(Figure 1): Beijing-Tianjin-Hebei urban agglomeration (BTH), Yangtze River Delta urban agglomeration (YRD), Triangle of
Central China (TC), Greater Bay Area urban agglomeration (GBA), Chengdu-Chongqing urban agglomeration (CC), and
130 Northern Slope of Tianshan Mountains urban agglomeration (NSTM).

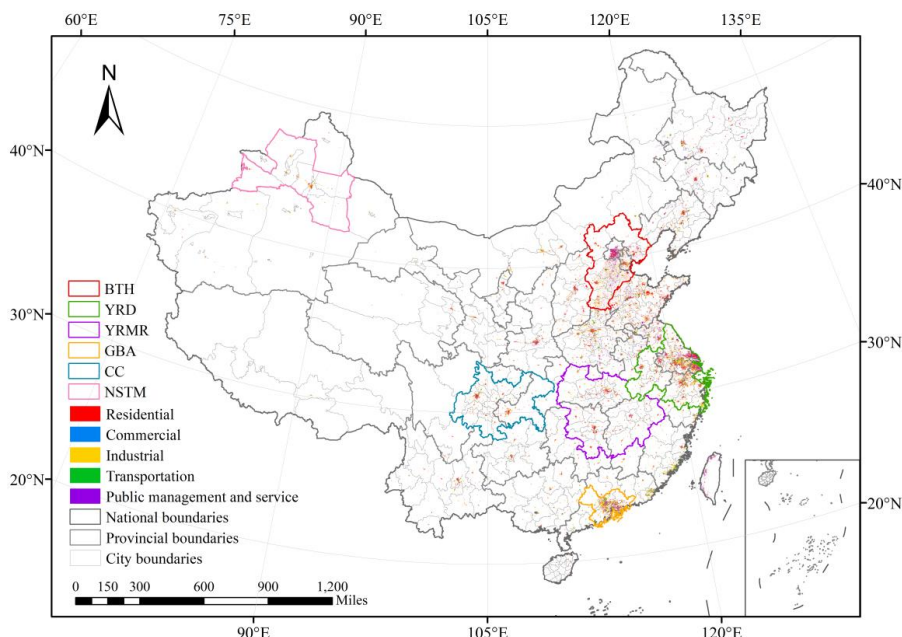


Figure 1. The location of study area and the distribution map of six major urban agglomerations. BTH: Beijing-Tianjin-Hebei
urban agglomeration; YRD: Yangtze River Delta urban agglomeration; TC: Triangle of Central China; GBA: Greater Bay Area
135 urban agglomeration; CC: Chengdu-Chongqing urban agglomeration; NSTM: Northern Slope of Tianshan Mountains urban
agglomeration.

2.2 Data sources

The hourly observation data of pollutants from national air quality control stations during 2017-2022 used in this study were
140 derived from urban air quality monitoring data released by the Ministry of Ecology and Environment of China
(<http://beijingair.sinaapp.com>). The data covers 1,482 sites across 336 prefecture-level cities in China and includes hour-by-hour mass concentrations of six pollutants (PM_{2.5}, PM₁₀, SO₂, NO₂, O₃, and CO).

The urban functional zone data comes from the 2018 China Basic Urban Land Use Type Map (EULUC-China) dataset
(<http://data.ess.tsinghua.edu.cn>). This map is based on the comprehensive use of 30-meter city contour data, OpenStreetMap
145 road network data, multi-source remote sensing data, night light data, and social big data (Autonavi POI number and Tencent
positioning population change characteristics) to determine the classification characteristics of urban plot scale, and the random
forest algorithm is used to draw. China's cities are divided into five functional zones: residential zone, commercial zone,
industrial zone, transportation zone, and public management and service zone (Gong et al., 2020).

The national Digital Elevation Model (DEM) data comes from the global DEM dataset released by the General Bathymetric
150 Chart of the Oceans (GEBCO) in 2022 (https://www.gebco.net/data_and_products/). This dataset includes global DEM data



from grid scale to basin scale, covering sea level change and ocean topography, etc. Grid DEM is combined with high-resolution satellite remote sensing images, and the global land and ocean areas are divided. DEM data is raster data with a spatial resolution of 500 meters.

2.3 Data analysis methods

155 2.3.1 Data preprocessing

The hourly concentration data of pollutants in the site were screened and cleaned, and the abnormal values and missing values in the data were eliminated. The minimum validity requirements of pollutant concentration data stipulated in Ambient Air Quality Standards (GB3095-2012) (<https://www.mee.gov.cn/>) shall be strictly followed during data processing, and data quality control shall be adopted to ensure the validity and reliability of atmospheric pollutant concentration data. Specific 160 methods are as follows (Li et al., 2019a; Silver et al., 2018; Yu et al., 2024):

- 1) Any concentration per hour value that is missing or less than or equal to zero is considered invalid data.
- 2) Each monitoring site should have an effective concentration value for at least 20 hours in a day. If a site has less than 20 active hours on a given day, the data for that day is considered invalid.
- 3) Each monitoring site should have at least 27 effective daily average concentration values in a month.
- 165 4) Each monitoring site should have at least 324 effective daily average concentration values in one year.
- 5) If the PM_{2.5} concentration of a station is greater than PM₁₀ for an hour, the data for that hour will be considered invalid.

2.3.2 Data analysis process

Initially, ArcGIS was employed to overlay the latitude and longitude data of the sites with the urban functional area data, allowing for the identification of the functional area category for each site through spatial connections. This process facilitated 170 the addition of new functional area attribute information to the site data. Subsequently, MATLAB was utilized to write code for batch processing the pre-processed pollutant concentration data from the sites, enabling the calculation of daily, monthly, and annual mean values for six pollutants at each site (Fan et al., 2020). Each functional area was then analyzed, establishing a site index for each functional area. The corresponding pollutant concentration data for each functional area was extracted based on this site index, leading to the classification of pollutant concentration data across different functional zones. Finally, 175 the average concentrations of the six pollutants within each functional area were computed across various spatial scales, including six geographical regions, six urban agglomerations, and three key regions. Using a similar methodology, the longitude and latitude data were overlaid with DEM grid data to obtain elevation information for each station, allowing for the calculation of mean pollutant concentrations for each functional area at different altitudes.

3 Results and discussion

180 3.1 Number of sites in different functional zones

Following the superposition analysis of the functional area and site latitude and longitude data, it is discovered that 118 sites are unrelated to any functional area and that 1364 sites in total overlap with the functional area. 1364 sites that coincide with functional zones are thus chosen for analysis in this research. In general, the majority of the sites are concentrated in public management and service and residential zone; of them, 555 are in public management and service zone , 320 are in residential 185 zone, and just 69 are on transportation zone (Figure 2).

Suzhou and Qingdao have the most residential zone sites, with 13 sites (Figure 2a); Jinan, Yantai, and Ganzhou have the most commercial zone sites, with 3 sites (Figure 2b); Weihai City has the most industrial zone sites, with 5 sites (Figure 2c); Bazhong, Guang'an, and Luohe have the most traffic sites, with 4 sites (Figure 2d). Hefei, Changsha, and Shenzhen have the largest number of public management and service zone sites, reaching 6 (Figure 2e). In addition, four cities—Longnan, Qamdo, Garze



190 Tibetan Autonomous Prefecture, Qiannan Buyi and Miao Autonomous Prefecture—do not have functional zone sites (Figure 2).

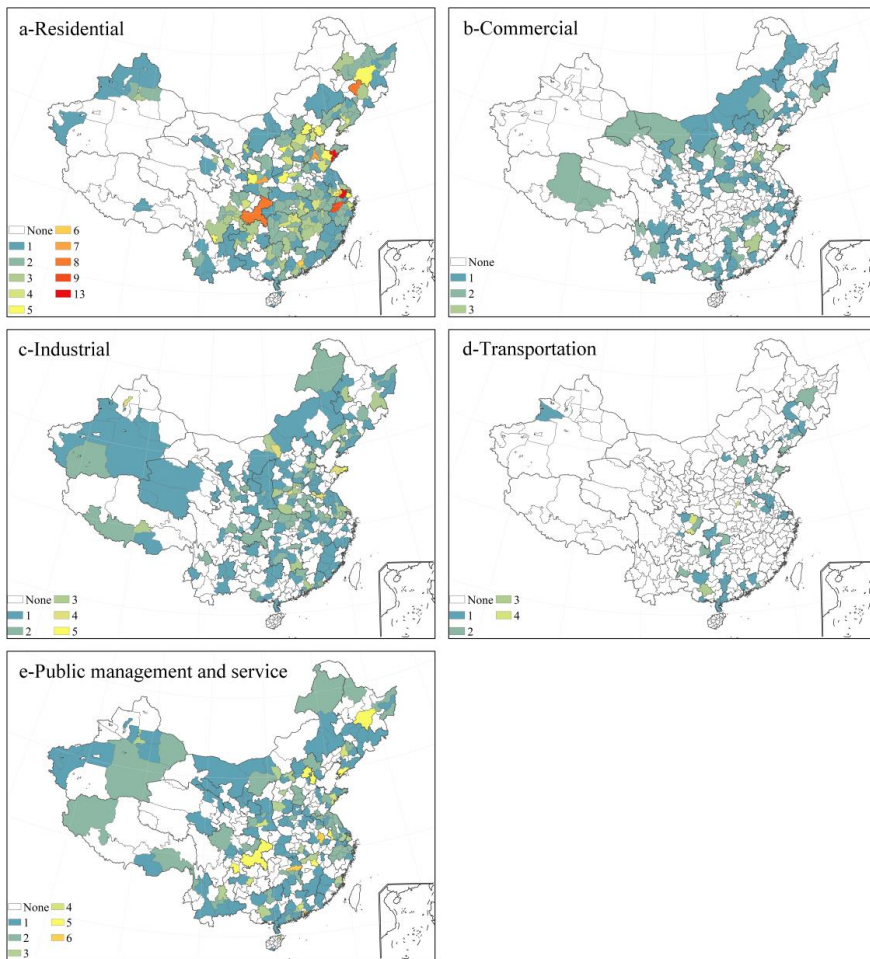


Figure 2. Statistics on the number of stations in different functional zones of each city.

195

3.2 Temporal variation

3.2.1 Overall interannual variation

The annual trend of PM_{2.5}, PM₁₀, SO₂, NO₂, and CO concentrations in various functional zones of Chinese cities is illustrated in Figure 3. From a nationwide perspective, there has been a consistent year-on-year decline in the concentrations of these 200 pollutants from 2017 to 2022. Specifically, PM_{2.5}, PM₁₀, NO₂, and CO concentrations decreased by 33.7%, 32.9%, 31.9%, and 33.6% respectively across Chinese cities as a whole. Compared with other pollutants, the concentration of SO₂ has the largest decrease, with a decrease rate of up to 53.5% (Figure 3c). This is due to China's emission reduction measures for air pollution control and loose coal control in recent years, which led to a continuous decline in SO₂ emissions (He et al., 2023b; Huang et al., 2021b). However, O₃ concentration showed a downward trend from 2018 to 2021, and then rebounded in 2022. Compared 205 with 2017, O₃ concentration decreased by 5.6% in 2021 and increased by 3.7% in 2022 (Figure 3e). In recent years, NO_x emissions in China have decreased significantly, while VOCs have decreased slightly. Due to the highly nonlinear response



relationship between O_3 and its precursors NO_x and VOCs, coupled with the influence of meteorological conditions, ozone concentration has increased (Lu et al., 2021; Wang et al., 2013; You et al., 2017).

Significant variations are observed in the reduction of pollutant concentrations across different functional zones. Except for

210 O_3 , the concentration of pollutants has improved most significantly in residential, commercial, and industrial areas. Compared with 2017, $PM_{2.5}$ concentration had decreased by 34.3%, 35.5%, and 33.8% in these areas by 2022, and SO_2 concentration had decreased by 55.6%, 56.4%, and 53.4%, respectively. The main reason is that following the implementation of policies such as the "Clean Winter Heating Plan for Northern China (2017–2021)" (NDRC, 2017) and the "Three-Year Action Plan for Winning the Blue Sky Defense Battle", the government intensified control over industrial pollution, promoted clean production
215 in enterprises, implemented clean heating measures in residential areas, and encouraged the use of clean fuels like natural gas and electricity (Song et al., 2023; Wang et al., 2022b). However, the rate of decrease in pollutant concentration in transportation zone was significantly lower than in other areas, with NO_2 showing the least reduction at 28.3% and an average annual decrease of $1.72\mu\text{g}/\text{m}^3$, indicating the slowest improvement. Road traffic is the primary source of NO_2 pollution (Xin et al., 2021). Although China has continued to implement initiatives to transform to cleaner automobiles to reduce traffic emissions of NO_2 ,
220 further efforts are required. In contrast to other pollutants, O_3 concentration has seen a significant rebound in residential, commercial, and transportation areas with high population activity, with an increase rate of 5.53%, 3.97%, and 4.01% in 2022, respectively, while in industrial areas, the rebound was minimal at only 2.64%. An increasing number of studies have shown that long-term exposure to O_3 pollution can adversely affect human health, potentially causing diseases of the nervous and respiratory systems, and even leading to premature death (He et al., 2023a; Li et al., 2022a; Yim et al., 2019). Therefore, 225 reducing ozone concentration, particularly in densely populated areas, is imperative.

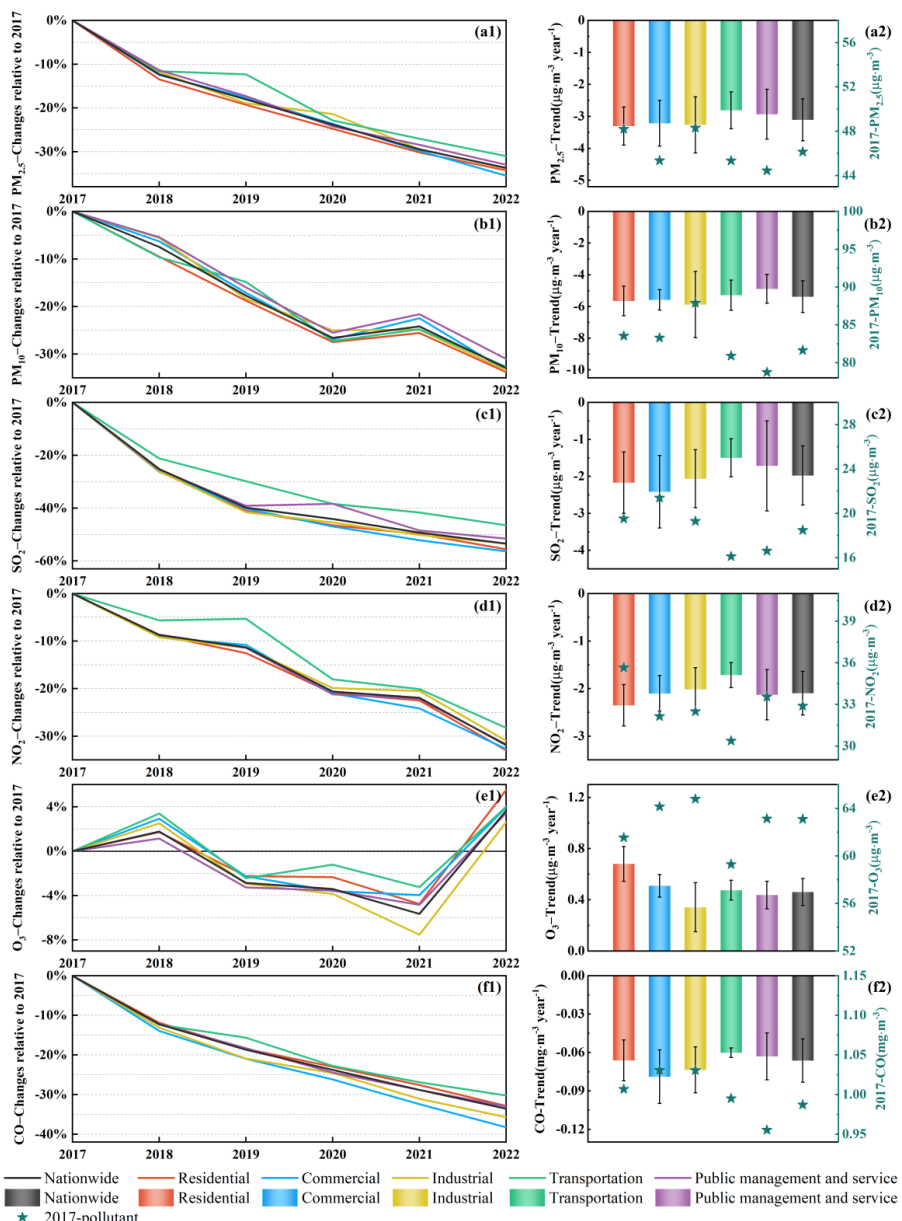


Figure 3. Annual trend of six pollutant concentrations in various functional zones of Chinese cities. (a1) and (a2) for $\text{PM}_{2.5}$, (b1) and (b2) for PM_{10} , (c1) and (c2) for SO_2 , (d1) and (d2) for NO_2 , (e1) and (e2) for O_3 , (f1) and (f2) for CO .

230

3.2.2 Seasonal variation

Based on the national seasonal changes (Figure 4 and Figure S1), the concentrations of $\text{PM}_{2.5}$, PM_{10} , SO_2 , NO_2 , and CO exhibited a U-shaped distribution from January to December, with higher concentrations observed in winter compared to summer. The high concentration of $\text{PM}_{2.5}$ in winter in China can be attributed to coal-burning heating in northern China, and 235 meteorological conditions that are not conducive to the diffusion of pollutants (winter temperature inversion, more stable atmospheric conditions, less wet deposition) also contribute to the accumulation of air pollutants (Fan et al., 2021; Wang et al., 2017). In contrast to other pollutants, O_3 displayed an inverted U-shaped seasonal variation with higher concentrations in



summer than in winter. This finding aligns with previous studies by Wang et al. (2022c) and Fan et al. (2020). The increased atmospheric temperature, intensified solar radiation, and extended sunshine duration during summer facilitate enhanced 240 photochemical reactions leading to heightened O₃ generation (Barzeghar et al., 2020).

Overall, the seasonal fluctuations of the six pollutants showed a downward trend from 2017 to 2022. The seasonal fluctuation of SO₂ and CO showed a decreasing trend year by year, and the difference of SO₂ and CO decreased from 22.8µg/m³ to 3.9µg/m³, and from 0.72mg/m³ to 0.43mg/m³. This downward trend can be attributed to the adjustment of China's energy structure and the implementation and improvement of desulfurization technology. In recent years, with the gradual reduction 245 of dependence on high-emission energy (such as coal), the shift to clean energy, and the continuous improvement of energy efficiency, the emission reduction of SO₂ and CO has achieved remarkable results, and the seasonal differences have also decreased (Qian et al., 2020). Specifically, SO₂ has the most significant decline in commercial zone, with a decrease of 85.2%. Commercial zone mainly includes shops, restaurants, etc., whose main emission sources may come from the coal or gas of small heating facilities and cooking equipment. After the implementation of environmental protection policies and 250 technological improvements, the SO₂ emissions of these emission sources have been significantly reduced. CO emissions from industrial zone experienced the most significant decrease, dropping by 42.4%. These emissions primarily arise from combustion, chemical reactions, and various industrial production processes. Following improvements in cleaner production methods and emission control technologies, CO emissions have also been further reduced. NO₂ and O₃ show the least variation in seasonal fluctuation, particularly in areas designated as public management and service zone. This stability can be attributed 255 to the scarcity of pollutant emission sources in public management and service zone, as well as the stringent environmental monitoring and management practices that are implemented.

The seasonal fluctuations of various pollutants in different functional zones exhibit significant disparities. For instance, the seasonal fluctuation of particulate matter (PM_{2.5} and PM₁₀) in industrial and transportation zones is notably higher than that in other functional zones. The seasonal fluctuation of PM_{2.5}(PM₁₀) in industrial and transportation zones is 50.5µg/m³ (66.1µg/m³) 260 and 51.0µg/m³ (65.7µg/m³), respectively. The primary cause of these seasonal changes is the variation in particulate matter concentration within the environment, particularly when there is low removal efficiency of industrial dust with high emissions, leading to an increase in this seasonal trend accordingly (Li et al., 2022b; Luo et al., 2022). Thus, the emission levels of particulate matter from industrial and transportation zones surpass those from other functional zones, resulting in conspicuous seasonal fluctuations. The greater seasonal fluctuation of NO₂ and O₃ observed in residential zone and industrial zone compared 265 to other functional zones can be attributed to activities such as heating and coal burning during winter, which elevate the production of nitrogen oxides along with ozone precursors within the atmosphere (Huang et al., 2013). Additionally, CO in industrial zone exhibited a significantly larger seasonal fluctuation at 0.59mg/m³ compared to other functional zones. In summary, it can be concluded that the largest variations among various pollutants occur in industrial zone, while public management and service zone experiences minimal fluctuations.

270

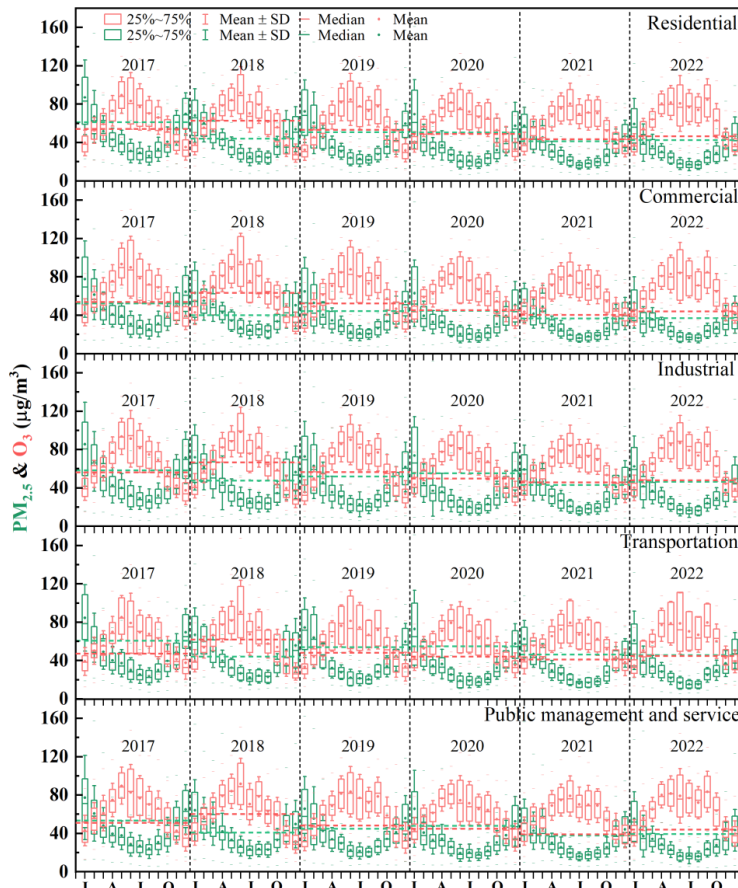
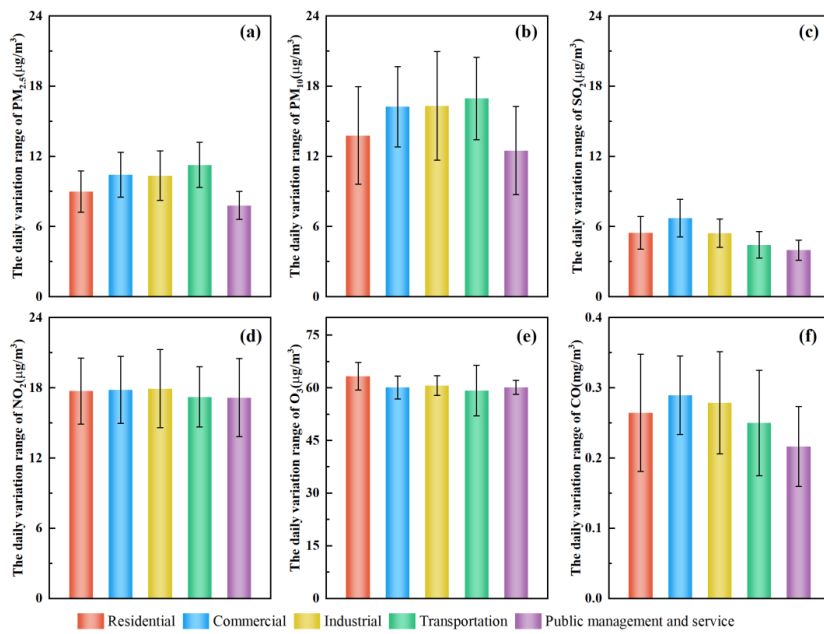


Figure 4. Seasonal variation trend of $\text{PM}_{2.5}$ and O_3 concentrations in various functional zones of Chinese cities. The dashed lines indicate the difference between the highest and lowest monthly mean concentration in the corresponding year.

275 As depicted in Figure 5 and Figure S2, the daily variation amplitude of different functional zones for NO_2 and O_3 exhibits minimal differences, significantly lower compared to the other four pollutants. Given that ozone is a regional pollutant, the variations among different functional zones are relatively small (Wang et al., 2022a). The daily variation of particulate matter ($\text{PM}_{2.5}$ and PM_{10}) in transportation, industrial, and commercial zones is significantly greater than that in residential and public management and service zones. This disparity can be attributed to factors such as working hours and peak traffic periods.

280 Transportation, industrial, and commercial zones, which are heavily trafficked and populated during business hours and peak times, contribute to higher emissions of particulate matter and, consequently, exhibit greater daily variation (Song et al., 2019). In commercial zone, the daily variation of SO_2 and CO notably exceeds that of other functional zones, with levels reaching $6.74 \mu\text{g}/\text{m}^3$ and $0.29 \text{mg}/\text{m}^3$, respectively. The emissions from the catering industry's cooking processes, peaking during lunch and dinner hours, are a significant source of these pollutants (ElSharkawy and Ibrahim, 2022). Conversely, public management

285 and service zone, which includes government agencies, schools, and hospitals, shows the smallest daily variation in SO_2 and CO levels at $3.99 \mu\text{g}/\text{m}^3$ and $0.22 \text{ mg}/\text{m}^3$, respectively, due to minimal pollutant emissions. Overall, the daily variation of pollutants is most pronounced in commercial, industrial, and transportation zones, while public management and service zone exhibits the least variation.



290

Figure 5. Daily variation range of PM_{2.5} (a), PM₁₀ (b), SO₂ (c), NO₂ (d), O₃ (e), and CO (f) concentrations in various functional zones of Chinese cities.

3.3 Spatial variation

295 3.3.1 Six geographical regions

In North and Northwest China, the concentrations of PM_{2.5}, PM₁₀, SO₂, NO₂, and CO are notably high (as shown in Figure 6). Specifically, the concentrations of PM_{2.5} and PM₁₀ are 8.07 $\mu\text{g}/\text{m}^3$ and 28.2 $\mu\text{g}/\text{m}^3$ higher, respectively, than in other regions. This disparity can be attributed to North and Northwest China being the epicenter of China's traditional industrial base, endowed with abundant coal and mineral resources. The presence of numerous large-scale enterprises, including coal-fired power plants, the steel industry, and the non-ferrous metal industry, contributes to significant pollutant emissions. Furthermore, the reliance on coal combustion for heating during the winter months exacerbates pollutant emissions (Wang et al., 2014; Li et al., 2019b). In contrast, the eastern and northern parts of China exhibit elevated levels of O₃, with concentrations 6.84 $\mu\text{g}/\text{m}^3$ higher than those in other specified regions. The dense population and thriving industry in these areas result in a substantial emission of ozone precursors, particularly during the warmer seasons, the higher temperature in East and North China further promotes the photochemical reaction of O₃ (He et al., 2023a).

In North China, Northeast China, and East China, the concentration of various pollutants in transportation zone is notably higher than in other functional zones, while the concentration of various pollutants in public management and service zone is the lowest. This is attributed to the well-developed transportation networks, ongoing expansion of transportation infrastructure, and substantial vehicle ownership in these regions, which collectively contribute to elevated emissions of road traffic pollutants (Guo et al., 2022). In central and southern China, the concentrations of pollutants in commercial and industrial zones are comparatively higher, while transportation zone exhibits the lowest levels. For instance, the levels of PM_{2.5} and NO₂ in transportation zone are respectively 4.75 and 5.00 $\mu\text{g}/\text{m}^3$ lower than in other functional zones. This may be attributed to the larger and more dispersed areas of transportation zone in central and southern China, which often feature extensive greening and open spaces, which facilitate the dilution and dispersion of pollutants, leading to more dispersed traffic pollution (Hong and Jin, 2021; Magazzino and Mele, 2021). The O₃ concentrations in residential and transportation zones in southwest China



are the lowest, with a notable $8.42 \mu\text{g}/\text{m}^3$ reduction compared to other functional zones. This could be due to the lower emissions of nitrogen oxides and volatile organic compounds, thus limiting the generation of O_3 . In contrast, the concentrations of other pollutants in these two functional zones are the highest. However, no clear pattern of pollutant concentration is observed across different functional zones in Northwest China.

320 According to the pollution situation of the above functional zones, the focus of air pollution control in different regions is different. In North, Northeast, and East China, the primary focus of air quality management should be on transportation-related emissions. For Central and Southern China, the emphasis should shift towards catering services and industrial emissions. The Southwest region requires attention to both residential and transportation-related pollution sources. In contrast, Northwest China necessitates a comprehensive approach to air quality management, addressing multiple pollution sources simultaneously.

325

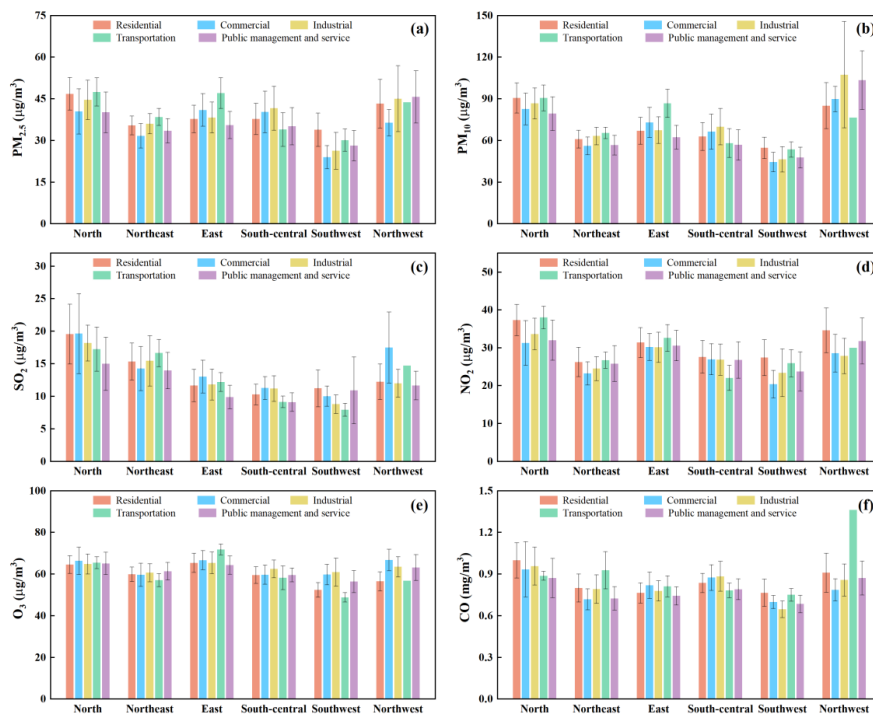


Figure 6. Concentrations of PM_{2.5} (a), PM₁₀ (b), SO₂ (c), NO₂ (d), O₃ (e), and CO (f) in each functional zone of the six geographical regions.

330 3.3.2 Six urban agglomerations

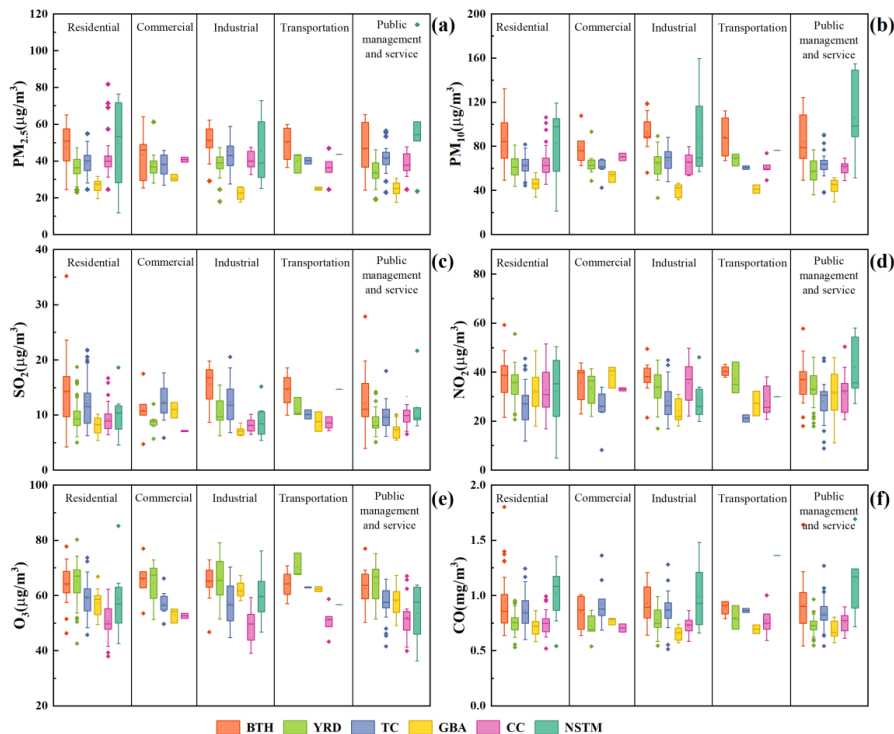
The Beijing-Tianjin-Hebei urban agglomeration (BTH) exhibits a pronounced high concentration of pollutants, as shown in Figure 7. BTH, recognized as the region with the highest pollutant emission intensity in China, experiences a climate characterized by static and stable weather conditions, weak winds, and a relatively low boundary layer height, which collectively provide favorable atmospheric conditions conducive to the formation and accumulation of pollutants (He et al.,

335 2020; Zhang and Cao, 2015). The Greater Bay Area (GBA) demonstrates significantly lower concentrations of PM_{2.5}, PM₁₀, and CO compared to the other urban agglomerations. Its proximity to the ocean and advantageous geographical positioning facilitate the dispersion of pollutants, resulting in a comparatively lower pollution level (Shen et al., 2019). The Yangtze River Delta urban agglomeration (YRD) records the highest concentration of O₃, exceeding $64.2 \mu\text{g}/\text{m}^3$, while the Chengdu-Chongqing urban agglomeration (CC) shows the lowest, with levels below $52.7 \mu\text{g}/\text{m}^3$. These findings corroborate the results



340 of Zhao et al. (Zhao et al., 2021b), highlighting the correlation between high population density and anthropogenic emissions of O_3 precursors in the YRD. The Northern Slope of Tianshan Mountain urban agglomeration (NSTM) is marked by elevated levels of particulate matter. Human activities and dust events contribute to the significant production of $PM_{2.5}$ and PM_{10} , with the high concentration of these particles being influenced by wind direction and speed (Luo et al., 2023).
 For BTH and YRD, the concentrations of pollutants in industrial and transportation zones are notably higher, particularly the
 345 NO_2 levels in transportation zone, which significantly surpass those in other functional zones, which are $40.5 \mu\text{g}/\text{m}^3$ and $37.0 \mu\text{g}/\text{m}^3$, respectively. This disparity is primarily attributed to the economic prosperity, dense population, and high-density traffic flow in these regions, with vehicle emissions identified as the predominant source of NO_2 (Yang et al., 2018). In the case of TC and CC, elevated pollutant levels are observed in commercial and industrial zones. The thriving catering industry in these regions, combined with the concentrated distribution of commercial and industrial zones resulting from topographical and
 350 planning constraints, contributes to a high emission intensity of pollutants per unit area (Liu et al., 2020). The GBA exhibits the lowest O_3 concentration in commercial zone, measured at $53.1 \mu\text{g}/\text{m}^3$, while other pollutants are highest in commercial zone. The higher concentration of various pollutants in NSTM's residential zone can be ascribed to the substantial use of loose coal burning from 2017 to 2022, resulting in substantial pollutant emissions.

In light of the varying pollution profiles within the aforementioned functional zones, the focus of atmospheric pollution
 355 mitigation in different urban agglomerations is different. BTH and YRD should focus on industrial and transportation zones. TC requires attention to commercial and industrial zones. Meanwhile, GBA should prioritize the mitigation of pollution on commercial zone.



360 **Figure 7.** Differences in concentrations of $PM_{2.5}$ (a), PM_{10} (b), SO_2 (c), NO_2 (d), O_3 (e), and CO (f) in each functional zone of the six urban agglomerations. BTH: Beijing-Tianjin-Hebei urban agglomeration; YRD: Yangtze River Delta urban agglomeration; TC: Triangle of Central China; GBA: Greater Bay Area urban agglomeration; CC: Chengdu-Chongqing urban agglomeration; NSTM: Northern Slope of Tianshan Mountains urban agglomeration.



365 **3.4 Analysis of influencing factors**

3.4.1 The impact of governance measures

Figure 8 shows the particulate matter in the Beijing-Tianjin-Hebei region and its surrounding areas has seen the greatest improvement, with $PM_{2.5}$ and PM_{10} concentrations decreasing by 10.5% and 9.8%, respectively. The improvement in SO_2 and CO in the Beijing-Tianjin-Hebei region and the Fen-Wei Plain is the most significant, with the SO_2 and CO concentrations in 370 the Beijing-Tianjin-Hebei region falling by 23.8% and 13.3%, respectively, and in the Fen-Wei Plain by 30.6% and 15.2%, respectively. The NO_2 levels in key areas are slightly better than those in non-key areas. These results indicate that since the implementation of the Three-Year Action Plan for Winning the Blue Sky Defense Battle, the air pollution control in key areas has achieved significant results.

The Beijing-Tianjin-Hebei region and its surrounding areas demonstrated the most significant improvement in transportation 375 zone for particulate matter ($PM_{2.5}$ and PM_{10}), with a reduction rate of 12.68% and 11.45%, respectively. However, commercial zone showed the least improvement, with a reduction rate of 9.28% for $PM_{2.5}$ and 8.34% for PM_{10} . This indicates that traffic areas in this region have achieved remarkable dust control. The improvement of transportation zone for gaseous pollutants (380 SO_2 , NO_2 , and CO) was the least significant, with decline rates of 16.72%, 7.08%, and 11.81%, respectively, suggesting that efforts to control automobile exhaust should be intensified in this region. In contrast, the Yangtze River Delta region saw the least improvement in particulate matter in transportation zone, while gaseous pollutants showed the greater improvement, indicating a need to strengthen dust control in this region's transportation zone. The industrial zone in Fen-Wei Plain has the 385 smallest improvement in the concentration of various pollutants, because it has abundant coal reserves and intensive energy industries (such as coal-fired power plants, iron and steel smelting, coal coking, etc.), resulting in more industrial pollutants and difficult improvement (Bai et al., 2021). The improvement in residential and commercial zone in other area is the greatest, while transportation zone has seen the least progress. It is clear that the Beijing-Tianjin-Hebei region and its surrounding areas, the Yangtze River Delta, and other area all need to enhance air pollution control in their transportation zone.

The rebound range of O_3 in three key areas is significantly higher than that in other area. The rebound rate of ozone in residential and public management and service zone is relatively large. The 1.9% increase in the O_3 rebound rate in residential 390 zone in the Fen-Wei Plain is particularly noteworthy. This increase in ozone can be attributed to the elevated levels of active oxygen-containing volatile organic compounds (OVOCs), especially the ongoing rise in formaldehyde (Lin et al., 2023). The aforementioned results indicate the necessity of promoting collaborative governance for $PM_{2.5}$ and O_3 .

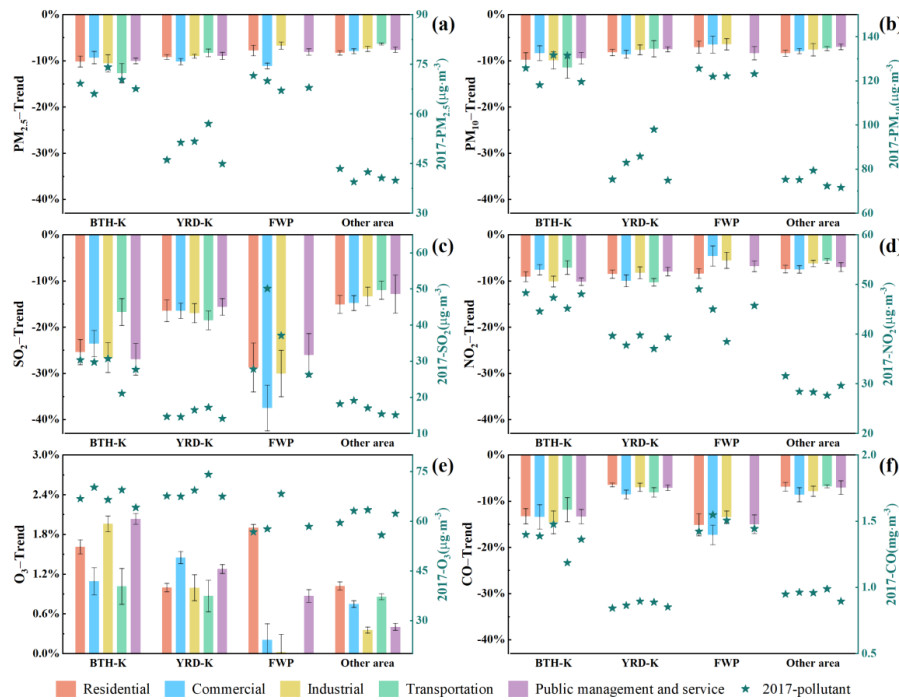


Figure 8. Annual variation trend of $\text{PM}_{2.5}$ (a), PM_{10} (b), SO_2 (c), NO_2 (d), O_3 (e), and CO (f) concentrations in various functional zones of the three key areas and other area. BTH-K: Beijing-Tianjin-Hebei region and its surrounding areas; YRD-K: Yangtze River Delta region; FWP: Fen-Wei Plain.

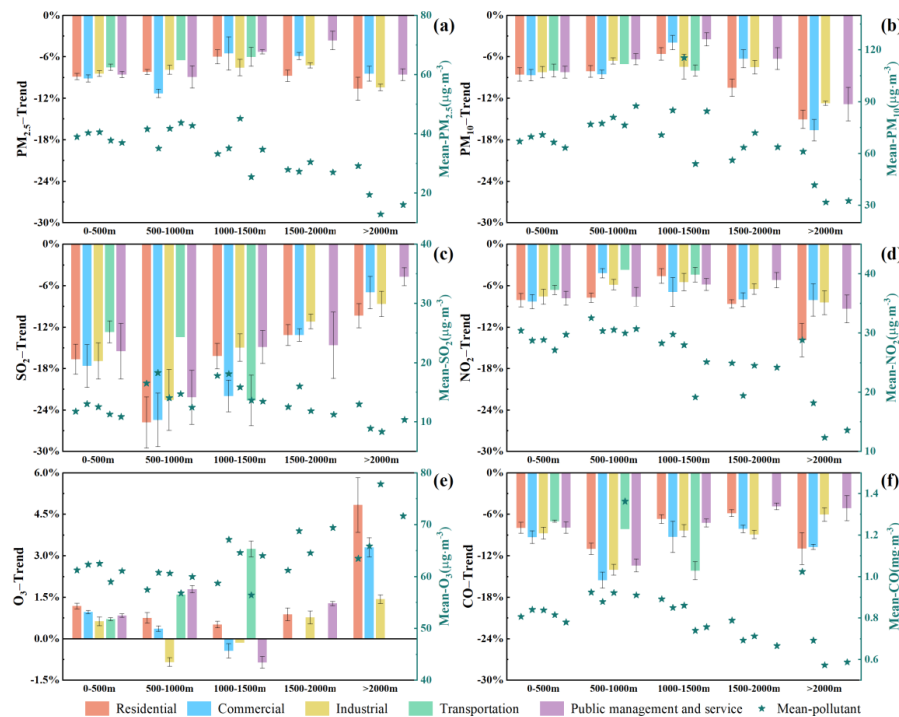
3.4.2 The impact of altitude

Figure 9 shows the average concentrations of $\text{PM}_{2.5}$, PM_{10} , SO_2 , NO_2 , and CO during 2017-2022 exhibit a general decrease with increasing altitude due to the predominant concentration of atmospheric pollution sources in China's lower eastern region. Additionally, within the boundary layer, convection movement lifts pollutant particles upward, leading to their dilution (Chen et al., 2024; Rohde and Muller, 2015). Conversely, the average concentration of O_3 increases with elevation and demonstrates a consistent relationship with altitude as previously observed by Ma et al. (2021). The reduction in SO_2 and CO concentrations at altitudes between 500 and 1000 m was notably greater than that at other altitudes. Similarly, improvements in PM_{10} and NO_2 concentrations above 2000 m were significantly greater compared to lower altitudes.

The reduction in particulate matter and NO_2 is most significant at high altitudes (above 2000 m), with diminishing improvements observed between 0-2000 m as altitude increases. Meanwhile, the improvement of SO_2 and CO decreases with the increase of altitude above 500 m.

In low-altitude regions (below 1000 m), the reduction of these pollutants in transportation zone was minimal. Conversely, in high-altitude regions (above 1500 m), a significant decrease in these pollutants was observed in both residential and industrial zones. This may be due to the higher density of vehicular traffic in lower altitude areas, coupled with reduced human activity in higher altitude regions.

O_3 rebounds more with the increase of altitude, especially in the high-altitude area above 2000 m. The possible reason is that global warming leads to a significant increase in the height of the atmospheric boundary layer, which promotes the transmission of O_3 from the upper air to the surface, resulting in a substantial rebound of O_3 (Liu et al., 2021). The higher the altitude, the more obvious the rebound will be. In particular, the O_3 concentration in residential zone has the largest rebound, up to 4.85%, which needs to be paid attention to.



420 **Figure 9.** Annual variation trend of PM_{2.5} (a), PM₁₀ (b), SO₂ (c), NO₂ (d), O₃ (e), and CO (f) concentrations in various functional zones at different altitudes.

3.4.3 The impact of working days

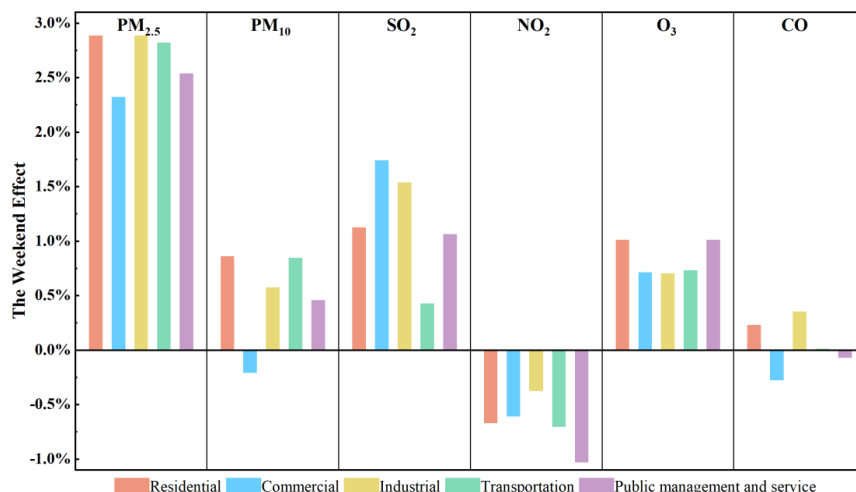
The weekend concentration greater than the weekday concentration is defined as the "positive weekend effect", and the 425 weekend concentration less than the weekday concentration is defined as the "negative weekend effect". The concentrations of PM_{2.5}, PM₁₀, SO₂, and O₃ on weekends are higher than those on weekdays, showing a "positive weekend effect" (Figure 10 and Figure S3). On the contrary, the concentration of NO₂ on weekends is smaller than that on weekdays, showing a "negative weekend effect". The average concentration of CO on weekdays and weekends is not much different, and the "weekend effect" is not obvious.

430 The phenomenon known as the "weekend effect" varies across distinct functional zones for each pollutant. For particulate matter (PM), a pronounced "positive weekend effect" is observed in residential, industrial, and transportation zones. The increased consumption of coal and biomass for residential living and the high proportion of people traveling on weekends lead to significantly higher particulate matter emissions from human activities on residential zone and transportation zone on weekends than on working days (Hua et al., 2021). In recent years, the influence of the pandemic and the implementation of 435 the industrial "off-peak production" policy have caused certain factories to operate normally on weekends, potentially contributing to the heightened weekend concentrations of PM in industrial zone. Regarding SO₂, the "positive weekend effect" is most pronounced in commercial zone, with weekend concentrations exceeding those of weekdays by 1.74%. This could be due to there being more SO₂ emissions from catering in commercial zone on weekends. In addition, the "negative weekend effect" for NO₂ is most pronounced in public management and service zone, where weekend concentrations are 1.03% lower 440 than those on weekdays. This reduction may be attributed to the fact that public management and service zone predominantly encompasses government institutions and educational facilities, where vehicular traffic and, consequently, NO₂ emissions from



vehicles, are significantly reduced during weekends (Zheng et al., 2023).

The "positive weekend effect" observed in the O_3 concentrations of residential and public management and service zones exceeds that of other functional zones, exhibiting an inverse trend in comparison to NO_2 exactly. This phenomenon corroborates the findings reported by (He, 2023), who identified a pronounced negative correlation between the weekly fluctuation patterns of NO_2 and O_3 . The formation process of O_3 in most areas of China is limited by volatile organic compounds (VOCs), and the reduction of NO_x emission can lead to the escalation in O_3 levels.



450 **Figure 10.** Weekend effect((weekend-weekday/weekday) of six pollutant concentrations in various functional zones nationwide.

4 Conclusion

Drawing on air quality observation data from 336 Chinese cities spanning the years 2017 to 2022, this study conducts a comprehensive analysis of the spatiotemporal evolution characteristics and potential influencing factors of air pollutants in various urban functional areas. The key findings are outlined below.

In terms of time scale, our analysis reveals a general downward trend in the concentrations of key air pollutants, especially in residential, commercial, and industrial zones, which can be largely attributed to the implementation of stringent national pollution control measures. This reduction is indicative of the effectiveness of these policies in combating air pollution.

460 However, ozone levels rebound notably in densely populated residential and commercial zones. The complex and fluctuating trend observed in ozone levels suggests that the management of this particular pollutant requires a more nuanced approach, considering its non-linear relationship with precursor emissions and meteorological conditions. especially in areas with high human activity such as residential, commercial, and transportation zones. Seasonal variation indicates a general downward trend in the fluctuation of these pollutants, with industrial zone showing the most pronounced seasonal variations and public management and service zone the least. Diurnal variation analysis reveals that commercial, industrial, and transportation zones experience the greatest daily fluctuations, in contrast to public management and service zone, which show minimal variation.

Spatial analysis revealed significant differences in pollutant concentrations in different regions and different functional zones. In North China, Northeast China, and East China, the concentration of various pollutants in transportation zone is higher than that in other functional zones. The concentration of pollutants in commercial and industrial zones is higher in central and southern China. The concentration of O_3 in residential and transportation zones in southwest China is the lowest, while the concentration of other pollutants in these two functional zones is the highest. Beijing-Tianjin-Hebei city cluster and Yangtze



River Delta city cluster are particularly prominent in the concentration of pollutants in industrial zone and transportation zone. The concentrations of pollutants in commercial zone and industrial zone in the middle reaches of Triangle of Central China and Chengdu-Chongqing city cluster are also relatively elevated.

475 The study also found that treatment measures, altitude, and working days have an impact on the concentration of pollutants in different functional zones. Overall, the improvement of pollutants in key areas implementing stricter air pollution control measures is greater than that in other areas. Nevertheless, it is imperative for all areas to enhance air pollution control in their transportation zone. The rebound rate of O₃ in key areas is significantly greater than that in other area, especially in residential zone and public management and service zone. The influence of altitude cannot be ignored. In low-altitude regions (below 480 1000 m), the reduction of these pollutants in transportation zone was minimal. Conversely, in high-altitude regions (above 1500 m), a significant decrease in these pollutants was observed in both residential and industrial zones.

The "weekend effect" for pollutants varies by functional zones. For particulate matter, a strong "weekend effect" is seen in residential and transportation zones due to increased human activities in these zones. SO₂ shows a notably "weekend effect" in commercial areas, likely due to increased emissions from catering. O₃ shows a "weekend effect", especially in residential 485 and public management and service zones, contrasting with the NO₂ trend. This finding underscores the importance of considering the unique activities and emission sources within each functional zone when developing air quality management strategies. Specifically, in residential zones, the heart of urban living, show a notable influence on ozone levels, particularly during the warm seasons. It highlights the need for cleaner domestic energy sources and energy-efficient housing to curb the emissions that contribute to ozone formation. For commercial zones, hubs of economic transactions and social activities, 490 exhibit a distinct "weekend effect," with increased emissions due to heightened activities. This finding calls for effective management of commercial operations, especially during peak times, and the potential for greener business practices.

To sum up, the intricate link between urbanization and air quality, highlighting the need for continuous monitoring and the development of zone-specific air quality strategies. The findings advocate for adaptive urban planning that takes into account the unique challenges posed by urban functional zones and the necessity for innovative pollution mitigation approaches. In 495 essence, the research contributes to a deeper understanding of the complex dynamics of air quality in urban China. It offers valuable guidance for policymakers and urban planners in crafting effective and targeted air quality management strategies, which are essential for achieving sustainable urban environments. The insights gained from this study are not only pertinent to China but also provide a framework for understanding urban air quality challenges and developing appropriate responses in other urban areas globally.

500 **Data availability.** All data needed to evaluate the conclusions in the paper are present in the paper and/or the Supplement. Also, all data used in the study are available from the corresponding author upon request.

Supplement. The supplement related to this article is available online at:

Author contributions. All authors made substantial contributions to this work. **Lulu Yuan:** Methodology, Visualization, Formal analysis, Resources, Data curation, Writing – original draft. **Wenchao Han:** Conceptualization, Methodology, Visualization, Resources, Writing – review & editing, Supervision. **Jiachen Meng:** Visualization, Data curation, Writing – review & editing. **Yang Wang:** Visualization, Writing – review & editing, Supervision. **Haojie Yu and Wenze Li:** Data curation, Writing – review & editing.

Competing interests. The authors declare that they have no conflict of interest.

Acknowledgements. This work was supported by the National Key Research and Development Program of China 510 (2022YFC3703004) and the National Natural Science Foundation of China (42301093).



References

Bai, X., Tian, H., Liu, X., Wu, B., Liu, S., Hao, Y., Luo, L., Liu, W., Zhao, S., Lin, S., Hao, J., Guo, Z., and Lv, Y.: Spatial-temporal variation characteristics of air pollution and apportionment of contributions by different sources in Shanxi province of China, *Atmos. Environ.*, 244, 117926, <https://doi.org/10.1016/j.atmosenv.2020.117926>, 2021.

515 Ban, Y., Liu, X., Yin, Z., Li, X., Yin, L., and Zheng, W.: Effect of urbanization on aerosol optical depth over Beijing: Land use and surface temperature analysis, *Urban Clim.*, 51, 101655, <https://doi.org/10.1016/j.uclim.2023.101655>, 2023.

Barzeghar, V., Sarbakhsh, P., Hassanvand, M. S., Faridi, S., and Gholampour, A.: Long-term trend of ambient air PM10, PM2.5, and O₃ and their health effects in Tabriz city, Iran, during 2006–2017, *Sustain. Cities Soc.*, 54, 101988, <https://doi.org/10.1016/j.scs.2019.101988>, 2020.

520 Berg, C. D., Schiller, J. H., Boffetta, P., Cai, J., Connolly, C., Kerpel-Fronius, A., Kitts, A. B., Lam, D. C. L., Mohan, A., Myers, R., Suri, T., Tammemagi, M. C., Yang, D., and Lam, S.: Air Pollution and Lung Cancer: A Review by International Association for the Study of Lung Cancer Early Detection and Screening Committee, *J. Thorac. Oncol.*, 18, 1277–1289, <https://doi.org/10.1016/j.jtho.2023.05.024>, 2023.

Cao, C., Lee, X., Liu, S., Schultz, N., Xiao, W., Zhang, M., and Zhao, L.: Urban heat islands in China enhanced by haze pollution, *Nat. Commun.*, 7, 12509, <https://doi.org/10.1038/ncomms12509>, 2016.

525 Chen, H. and Sun, J.: Changes in Drought Characteristics over China Using the Standardized Precipitation Evapotranspiration Index, *J. Clim.*, 28, 5430–5447, <https://doi.org/10.1175/JCLI-D-14-00707.1>, 2015.

Chen, S. and Gong, B.: Response and adaptation of agriculture to climate change: Evidence from China, *J. Dev. Econ.*, 148, 102557, <https://doi.org/10.1016/j.jdeveco.2020.102557>, 2021.

530 Chen, X. and Wei, F.: Impact of territorial spatial landscape pattern on PM2.5 and O₃ concentrations in the Yangtze River delta urban agglomeration: Exploration and planning strategies, *J. Clean. Prod.*, 452, 142172, <https://doi.org/10.1016/j.jclepro.2024.142172>, 2024.

Chen, Z.-H., Li, B.-W., Li, B., Peng, Z.-R., Huang, H.-C., Wu, J.-Q., and He, H.-D.: Identification of particle distribution pattern in vertical profile via unmanned aerial vehicles observation, *Environ. Pollut.*, 348, 123893, <https://doi.org/10.1016/j.envpol.2024.123893>, 2024.

535 Cheng, Y., Liu, H., Wang, H., and Hao, Q.: Differentiated climate-driven Holocene biome migration in western and eastern China as mediated by topography, *Earth-Sci. Rev.*, 182, 174–185, <https://doi.org/10.1016/j.earscirev.2018.05.006>, 2018.

Deng, C., Tian, S., Li, Z., and Li, K.: Spatiotemporal characteristics of PM2.5 and ozone concentrations in Chinese urban clusters, *Chemosphere*, 295, 133813, <https://doi.org/10.1016/j.chemosphere.2022.133813>, 2022.

540 Dmitrienko, A., Lipovenko, M., Gostilovich, A., Kolosov, A., and Ming, L.: Development strategies of high-tech companies in China: Huawei and Tencent, *Nexo Rev. Científica*, 36, 176–187, <https://doi.org/10.5377/nexo.v36i02.16058>, 2023.

Dong, J., Liu, P., Song, H., Yang, D., Yang, J., Song, G., Miao, C., Zhang, J., and Zhang, L.: Effects of anthropogenic precursor emissions and meteorological conditions on PM2.5 concentrations over the “2+26” cities of northern China, *Environ. Pollut.*, 315, 120392, <https://doi.org/10.1016/j.envpol.2022.120392>, 2022.

545 Duan, S., Liu, Q., Jiang, D., Jiang, Y., Lin, Y., and Gong, Z.: Exploring the Joint Impacts of Natural and Built Environments on PM2.5 Concentrations and Their Spatial Heterogeneity in the Context of High-Density Chinese Cities, *Sustainability*, 13, 11775, <https://doi.org/10.3390/su132111775>, 2021.

ElSharkawy, M. F. and Ibrahim, O. A.: Impact of the Restaurant Chimney Emissions on the Outdoor Air Quality, *Atmosphere*, 13, 261, <https://doi.org/10.3390/atmos13020261>, 2022.

550 Fan, C., Tian, L., Zhou, L., Hou, D., Song, Y., Qiao, X., and Li, J.: Examining the impacts of urban form on air pollutant emissions: Evidence from China, *J. Environ. Manage.*, 212, 405–414, <https://doi.org/10.1016/j.jenvman.2018.02.001>, 2018a.

Fan, H., Zhao, C., and Yang, Y.: A comprehensive analysis of the spatio-temporal variation of urban air pollution in China during 2014–2018, *Atmos. Environ.*, 220, 117066, <https://doi.org/10.1016/j.atmosenv.2019.117066>, 2020.



Fan, H., Zhao, C., Yang, Y., and Yang, X.: Spatio-Temporal Variations of the PM2.5/PM10 Ratios and Its Application to Air
555 Pollution Type Classification in China, *Front. Environ. Sci.*, 9, <https://doi.org/10.3389/fenvs.2021.692440>, 2021.

Fan, J., Leung, L. R., Rosenfeld, D., Chen, Q., Li, Z., Zhang, J., and Yan, H.: Microphysical effects determine macrophysical
response for aerosol impacts on deep convective clouds, *Proc. Natl. Acad. Sci.*, 110, E4581–E4590,
<https://doi.org/10.1073/pnas.1316830110>, 2013.

Fan, J., Wu, L., Zhang, F., Cai, H., Wang, X., Lu, X., and Xiang, Y.: Evaluating the effect of air pollution on global and diffuse
560 solar radiation prediction using support vector machine modeling based on sunshine duration and air temperature, *Renew. Sustain. Energy Rev.*, 94, 732–747, <https://doi.org/10.1016/j.rser.2018.06.029>, 2018b.

Fang, C., Xue, K., Li, J., and Wang, J.: Characteristics and Weekend Effect of Air Pollution in Eastern Jilin Province, *Atmosphere*, 13, 681, <https://doi.org/10.3390/atmos13050681>, 2022.

Gong, P., Chen, B., Li, X., Liu, H., Wang, J., Bai, Y., Chen, J., Chen, X., Fang, L., Feng, S., Feng, Y., Gong, Y., Gu, H., Huang,
565 H., Huang, X., Jiao, H., Kang, Y., Lei, G., Li, A., Li, X., Li, X., Li, Y., Li, Z., Li, Z., Liu, C., Liu, C., Liu, M., Liu, S., Mao, W.,
Miao, C., Ni, H., Pan, Q., Qi, S., Ren, Z., Shan, Z., Shen, S., Shi, M., Song, Y., Su, M., Ping Suen, H., Sun, B., Sun, F., Sun,
J., Sun, L., Sun, W., Tian, T., Tong, X., Tseng, Y., Tu, Y., Wang, H., Wang, L., Wang, X., Wang, Z., Wu, T., Xie, Y., Yang, J.,
Yang, J., Yuan, M., Yue, W., Zeng, H., Zhang, K., Zhang, N., Zhang, T., Zhang, Y., Zhao, F., Zheng, Y., Zhou, Q., Clinton, N.,
Zhu, Z., and Xu, B.: Mapping essential urban land use categories in China (EULUC-China): preliminary results for 2018, *Sci.
570 Bull.*, 65, 182–187, <https://doi.org/10.1016/j.scib.2019.12.007>, 2020.

Guo, D., Dall'erba, S., and Gallo, J. L.: The Leading Role of Manufacturing in China's Regional Economic Growth: A Spatial
Econometric Approach of Kaldor's Laws, *Int. Reg. Sci. Rev.*, 36, 139–166, <https://doi.org/10.1177/0160017612457779>, 2013.

Guo, J., Deng, M., Lee, S. S., Wang, F., Li, Z., Zhai, P., Liu, H., Lv, W., Yao, W., and Li, X.: Delaying precipitation and
lightning by air pollution over the Pearl River Delta. Part I: Observational analyses, *J. Geophys. Res. Atmospheres*, 121, 6472–
575 6488, <https://doi.org/10.1002/2015JD023257>, 2016.

Guo, Y., Lu, Q., Wang, S., and Wang, Q.: Analysis of air quality spatial spillover effect caused by transportation infrastructure,
Transp. Res. Part Transp. Environ., 108, 103325, <https://doi.org/10.1016/j.trd.2022.103325>, 2022.

Han, W., Li, Z., Wu, F., Zhang, Y., Guo, J., Su, T., Cribb, M., Fan, J., Chen, T., Wei, J., and Lee, S.-S.: The mechanisms and
seasonal differences of the impact of aerosols on daytime surface urban heat island effect, *Atmospheric Chem. Phys.*, 20, 6479–
580 6493, <https://doi.org/10.5194/acp-20-6479-2020>, 2020.

He, C., Zhang, Y., Schneider, A., Chen, R., Zhang, Y., Ma, W., Kinney, P. L., and Kan, H.: The inequality labor loss risk from
future urban warming and adaptation strategies, *Nat. Commun.*, 13, 3847, <https://doi.org/10.1038/s41467-022-31145-2>, 2022.

He, C., Wu, Q., Li, B., Liu, J., Gong, X., and Zhang, L.: Surface ozone pollution in China: Trends, exposure risks, and drivers,
Front. Public Health, 11, <https://doi.org/10.3389/fpubh.2023.1131753>, 2023a.

He, C., Kumar, R., Tang, W., Pfister, G., Xu, Y., Qian, Y., and Brasseur, G.: Air Pollution Interactions with Weather and Climate
Extremes: Current Knowledge, Gaps, and Future Directions, *Curr. Pollut. Rep.*, <https://doi.org/10.1007/s40726-024-00296-9>,
2024.

He, J., Zhao, M., Zhang, B., Wang, P., Zhang, D., Wang, M., Liu, B., Li, N., Yu, K., Zhang, Y., Zhou, T., and Jing, B.: The
impact of steel emissions on air quality and pollution control strategy in Caofeidian, North China, *Atmospheric Pollut. Res.*,
590 11, 1238–1247, <https://doi.org/10.1016/j.apr.2020.04.012>, 2020.

He, R.-R.: Quantifying the weekly cycle effect of air pollution in cities of China, *Stoch. Environ. Res. Risk Assess.*, 37, 2445–
2457, <https://doi.org/10.1007/s00477-023-02399-z>, 2023.

He, T., Tang, Y., Cao, R., Xia, N., Li, B., and Du, E.: Distinct urban-rural gradients of air NO₂ and SO₂ concentrations in
response to emission reductions during 2015–2022 in Beijing, China, *Environ. Pollut.*, 333, 122021,
595 <https://doi.org/10.1016/j.envpol.2023.122021>, 2023b.

Hong, C. and Jin, X.: Green change in the core build-up areas of China: Information from MODIS data, *Ecol. Indic.*, 122,
596 20–30, <https://doi.org/10.1016/j.ecolind.2022.107350>, 2023.



107270, <https://doi.org/10.1016/j.ecolind.2020.107270>, 2021.

Hua, J., Zhang, Y., de Foy, B., Mei, X., Shang, J., and Feng, C.: Competing PM2.5 and NO₂ holiday effects in the Beijing area vary locally due to differences in residential coal burning and traffic patterns, *Sci. Total Environ.*, 750, 141575, 600 <https://doi.org/10.1016/j.scitotenv.2020.141575>, 2021.

Huang, J., Zhou, C., Lee, X., Bao, Y., Zhao, X., Fung, J., Richter, A., Liu, X., and Zheng, Y.: The effects of rapid urbanization on the levels in tropospheric nitrogen dioxide and ozone over East China, *Atmos. Environ.*, 77, 558–567, 600 <https://doi.org/10.1016/j.atmosenv.2013.05.030>, 2013.

Huang, Q., Xu, C., Jiang, W., Yue, W., Rong, Q., Gu, Z., and Su, M.: Urban compactness and patch complexity influence 605 PM2.5 concentrations in contrasting ways: Evidence from the Guangdong-Hong Kong-Macao Greater Bay Area of China, *Ecol. Indic.*, 133, 108407, <https://doi.org/10.1016/j.ecolind.2021.108407>, 2021a.

Huang, R., Ju, T., Dong, H., Duan, J., Fan, J., Liang, Z., and Geng, T.: Analysis of atmospheric SO₂ in Sichuan-Chongqing 600 region based on OMI data, *Environ. Monit. Assess.*, 193, 849, <https://doi.org/10.1007/s10661-021-09638-2>, 2021b.

Huszar, P., Karlický, J., Bartík, L., Liaskoni, M., Prieto Perez, A. P., and Šindelářová, K.: Impact of urbanization on gas-phase 610 pollutant concentrations: a regional-scale, model-based analysis of the contributing factors, *Atmospheric Chem. Phys.*, 22, 12647–12674, <https://doi.org/10.5194/acp-22-12647-2022>, 2022.

Kuerban, M., Waili, Y., Fan, F., Liu, Y., Qin, W., Dore, A. J., Peng, J., Xu, W., and Zhang, F.: Spatio-temporal patterns of air 600 pollution in China from 2015 to 2018 and implications for health risks, *Environ. Pollut.*, 258, 113659, <https://doi.org/10.1016/j.envpol.2019.113659>, 2020.

615 Li, F. and Zhou, T.: Effects of urban form on air quality in China: An analysis based on the spatial autoregressive model, *Cities*, 89, 130–140, <https://doi.org/10.1016/j.cities.2019.01.025>, 2019.

Li, J., Lu, H., Cao, M., Tong, M., Wang, R., Yang, X., Liu, H., Xiao, Q., Chao, B., Liu, Y., Xue, T., and Guan, T.: Long-Term 610 Exposure to Ozone Increases Neurological Disability after Stroke: Findings from a Nationwide Longitudinal Study in China, *Biology*, 11, 1216, <https://doi.org/10.3390/biology11081216>, 2022a.

620 Li, K., Jacob, D. J., Liao, H., Shen, L., Zhang, Q., and Bates, K. H.: Anthropogenic drivers of 2013–2017 trends in summer surface ozone in China, *Proc. Natl. Acad. Sci.*, 116, 422–427, <https://doi.org/10.1073/pnas.1812168116>, 2019a.

Li, K., Li, C., Liu, M., Hu, Y., Wang, H., and Wu, W.: Multiscale analysis of the effects of urban green infrastructure landscape 620 patterns on PM2.5 concentrations in an area of rapid urbanization, *J. Clean. Prod.*, 325, 129324, <https://doi.org/10.1016/j.jclepro.2021.129324>, 2021.

625 Li, R., Fu, H., Cui, L., Li, J., Wu, Y., Meng, Y., Wang, Y., and Chen, J.: The spatiotemporal variation and key factors of SO₂ in 336 cities across China, *J. Clean. Prod.*, 210, 602–611, <https://doi.org/10.1016/j.jclepro.2018.11.062>, 2019b.

Li, S., Zou, B., Ma, X., Liu, N., Zhang, Z., Xie, M., and Zhi, L.: Improving air quality through urban form optimization: A 630 review study, *Build. Environ.*, 243, 110685, <https://doi.org/10.1016/j.buildenv.2023.110685>, 2023.

Li, W., Yang, G., and Qian, X.: The socioeconomic factors influencing the PM2.5 levels of 160 cities in China, *Sustain. Cities 630 Soc.*, 84, 104023, <https://doi.org/10.1016/j.scs.2022.104023>, 2022b.

Li, X., Zhang, F., Ren, J., Han, W., Zheng, B., Liu, J., Chen, L., and Jiang, S.: Rapid narrowing of the urban–suburban gap in air 635 pollutant concentrations in Beijing from 2014 to 2019, *Environ. Pollut.*, 304, 119146, <https://doi.org/10.1016/j.envpol.2022.119146>, 2022c.

Li, Z., Rosenfeld, D., and Fan, J.: Aerosols and Their Impact on Radiation, Clouds, Precipitation, and Severe Weather Events, 640 in: *Oxford Research Encyclopedia of Environmental Science*, <https://doi.org/10.1093/acrefore/9780199389414.013.126>, 2017.

Lin, C., Huang, R.-J., Zhong, H., Duan, J., Wang, Z., Huang, W., and Xu, W.: Elucidating ozone and PM_{2.5} pollution in the 645 Fenwei Plain reveals the co-benefits of controlling precursor gas emissions in winter haze, *Atmospheric Chem. Phys.*, 23, 3595–3607, <https://doi.org/10.5194/acp-23-3595-2023>, 2023.

Liu, M. and Liu, H.: Influence of Climate Change on Carbon Emissions during Grain Production and Its Mechanism,



640 Sustainability, 15, 10237, <https://doi.org/10.3390/su151310237>, 2023.
Liu, M., Wei, D., and Chen, H.: Consistency of the relationship between air pollution and the urban form: Evidence from the COVID-19 natural experiment, Sustain. Cities Soc., 83, 103972, <https://doi.org/10.1016/j.scs.2022.103972>, 2022.

Liu, R., Shao, M., and Wang, Q.: Multi-timescale variation characteristics of PM2.5 in different regions of China during 2014–2022, Sci. Total Environ., 920, 171008, <https://doi.org/10.1016/j.scitotenv.2024.171008>, 2024.

645 Liu, Y., Zhang, X., Pan, X., Ma, X., and Tang, M.: The spatial integration and coordinated industrial development of urban agglomerations in the Yangtze River Economic Belt, China, Cities, 104, 102801, <https://doi.org/10.1016/j.cities.2020.102801>, 2020.

Liu, Y., Wang, T., Stavrakou, T., Elguindi, N., Doumbia, T., Granier, C., Bouarar, I., Gaubert, B., and Brasseur, G. P.: Diverse response of surface ozone to COVID-19 lockdown in China, Sci. Total Environ., 789, 147739, <https://doi.org/10.1016/j.scitotenv.2021.147739>, 2021.

Liu, Y., Geng, G., Cheng, J., Liu, Y., Xiao, Q., Liu, L., Shi, Q., Tong, D., He, K., and Zhang, Q.: Drivers of Increasing Ozone during the Two Phases of Clean Air Actions in China 2013–2020, Environ. Sci. Technol., 57, 8954–8964, <https://doi.org/10.1021/acs.est.3c00054>, 2023.

650 Lu, C., Mao, J., Wang, L., Guan, Z., Zhao, G., and Li, M.: An unusual high ozone event over the North and Northeast China during the record-breaking summer in 2018, J. Environ. Sci., 104, 264–276, <https://doi.org/10.1016/j.jes.2020.11.030>, 2021.

Luo, Y., Zhao, T., Yang, Y., Zong, L., Kumar, K. R., Wang, H., Meng, K., Zhang, L., Lu, S., and Xin, Y.: Seasonal changes in the recent decline of combined high PM2.5 and O3 pollution and associated chemical and meteorological drivers in the Beijing–Tianjin–Hebei region, China, Sci. Total Environ., 838, 156312, <https://doi.org/10.1016/j.scitotenv.2022.156312>, 2022.

655 Luo, Y., Xu, L., Li, Z., Zhou, X., Zhang, X., Wang, F., Peng, J., Cao, C., Chen, Z., and Yu, H.: Air pollution in heavy industrial cities along the northern slope of the Tianshan Mountains, Xinjiang: characteristics, meteorological influence, and sources, Environ. Sci. Pollut. Res., 30, 55092–55111, <https://doi.org/10.1007/s11356-023-25757-4>, 2023.

Ma, R., Ban, J., Wang, Q., Zhang, Y., Yang, Y., He, M. Z., Li, S., Shi, W., and Li, T.: Random forest model based fine scale spatiotemporal O3 trends in the Beijing–Tianjin–Hebei region in China, 2010 to 2017, Environ. Pollut., 276, 116635, <https://doi.org/10.1016/j.envpol.2021.116635>, 2021.

660 665 Magazzino, C. and Mele, M.: On the relationship between transportation infrastructure and economic development in China, Res. Transp. Econ., 88, 100947, <https://doi.org/10.1016/j.retrec.2020.100947>, 2021.

Mao, X., Wang, L., Pan, X., Zhang, M., Wu, X., and Zhang, W.: A study on the dynamic spatial spillover effect of urban form on PM2.5 concentration at county scale in China, Atmospheric Res., 269, 106046, <https://doi.org/10.1016/j.atmosres.2022.106046>, 2022.

670 Meng, J., Han, W., and Yuan, C.: Seasonal and multi-scale difference of the relationship between built-up land landscape pattern and PM2.5 concentration distribution in Nanjing, Ecol. Indic., 156, 111079, <https://doi.org/10.1016/j.ecolind.2023.111079>, 2023.

NDRC: Clean Winter Heating Plan for Northern China (2017–2021), National Development and Reform Commission, https://www.gov.cn/xinwen/2017-12/20/content_5248855.htm (last access: 7 August 2024), 2017 (in Chinese).

675 Ouyang, X., Wei, X., Li, Y., Wang, X.-C., and Klemeš, J. J.: Impacts of urban land morphology on PM2.5 concentration in the urban agglomerations of China, J. Environ. Manage., 283, 112000, <https://doi.org/10.1016/j.jenvman.2021.112000>, 2021.

Qi, G., Wang, Z., Wei, L., and Wang, Z.: Multidimensional effects of urbanization on PM2.5 concentration in China, Environ. Sci. Pollut. Res., 29, 77081–77096, <https://doi.org/10.1007/s11356-022-21298-4>, 2022.

680 Qi, G., Che, J., and Wang, Z.: Differential effects of urbanization on air pollution: Evidences from six air pollutants in mainland China, Ecol. Indic., 146, 109924, <https://doi.org/10.1016/j.ecolind.2023.109924>, 2023.

Qian, Y., Scherer, L., Tukker, A., and Behrens, P.: China's potential SO2 emissions from coal by 2050, Energy Policy, 147, 111856, <https://doi.org/10.1016/j.enpol.2020.111856>, 2020.



Qian, Y., Chakraborty, T. C., Li, J., Li, D., He, C., Sarangi, C., Chen, F., Yang, X., and Leung, L. R.: Urbanization Impact on Regional Climate and Extreme Weather: Current Understanding, Uncertainties, and Future Research Directions, *Adv. Atmospheric Sci.*, 39, 819–860, <https://doi.org/10.1007/s00376-021-1371-9>, 2022.

685 Qin, Y., Li, J., Gong, K., Wu, Z., Chen, M., Qin, M., Huang, L., and Hu, J.: Double high pollution events in the Yangtze River Delta from 2015 to 2019: Characteristics, trends, and meteorological situations, *Sci. Total Environ.*, 792, 148349, <https://doi.org/10.1016/j.scitotenv.2021.148349>, 2021.

Qin, Y., Sun, C., Li, D., Zhang, H., Wang, H., and Duan, Y.: Does urban air pollution have an impact on public health? Empirical evidence from 288 prefecture-level cities in China, *Urban Clim.*, 51, 101660, <https://doi.org/10.1016/j.uclim.2023.101660>, 2023.

Rohde, R. A. and Muller, R. A.: Air Pollution in China: Mapping of Concentrations and Sources, *PLOS ONE*, 10, e0135749, <https://doi.org/10.1371/journal.pone.0135749>, 2015.

Rosenfeld, D., Lohmann, U., Raga, G. B., O'Dowd, C. D., Kulmala, M., Fuzzi, S., Reissell, A., and Andreae, M. O.: Flood or 695 Drought: How Do Aerosols Affect Precipitation?, *Science*, 321, 1309–1313, <https://doi.org/10.1126/science.1160606>, 2008.

Shen, H., Tao, S., Chen, Y., Ciais, P., Güneralp, B., Ru, M., Zhong, Q., Yun, X., Zhu, X., Huang, T., Tao, W., Chen, Y., Li, B., Wang, X., Liu, W., Liu, J., and Zhao, S.: Urbanization-induced population migration has reduced ambient PM2.5 concentrations in China, *Sci. Adv.*, 3, e1700300, <https://doi.org/10.1126/sciadv.1700300>, 2017.

Shen, Y., Zhang, L., Fang, X., Ji, H., Li, X., and Zhao, Z.: Spatiotemporal patterns of recent PM2.5 concentrations over typical 700 urban agglomerations in China, *Sci. Total Environ.*, 655, 13–26, <https://doi.org/10.1016/j.scitotenv.2018.11.105>, 2019.

Shen, Z., Zhang, Z., Cui, L., Xia, Z., and Zhang, Y.: Coordinated change of PM2.5 and multiple landscapes based on spatial coupling model: Comparison of inland and waterfront cities, *Environ. Impact Assess. Rev.*, 102, 107194, <https://doi.org/10.1016/j.eiar.2023.107194>, 2023.

Silver, B., Reddington, C. L., Arnold, S. R., and Spracklen, D. V.: Substantial changes in air pollution across China during 705 2015–2017, *Environ. Res. Lett.*, 13, 114012, <https://doi.org/10.1088/1748-9326/aae718>, 2018.

Song, C., Liu, B., Cheng, K., Cole, M. A., Dai, Q., Elliott, R. J. R., and Shi, Z.: Attribution of Air Quality Benefits to Clean Winter Heating Policies in China: Combining Machine Learning with Causal Inference, *Environ. Sci. Technol.*, 57, 17707–17717, <https://doi.org/10.1021/acs.est.2c06800>, 2023.

Song, J., Zhao, C., Lin, T., Li, X., and Prishchepov, A. V.: Spatio-temporal patterns of traffic-related air pollutant emissions in 710 different urban functional zones estimated by real-time video and deep learning technique, *J. Clean. Prod.*, 238, 117881, <https://doi.org/10.1016/j.jclepro.2019.117881>, 2019.

SC: Notice of the general office of the state council on issuing the air pollution prevention and control action plan, State Council of the People's Republic of China, https://www.gov.cn/gongbao/content/2013/content_2496394.htm (last access: 7 August 2024), 2013 (in Chinese).

715 SC: Notice of the general office of the state council on issuing the three-year action plan for winning the blue sky defense battle, State Council of the People's Republic of China, https://www.gov.cn/zhengce/content/2018-07/03/content_5303158.htm (last access: 7 August 2024), 2018 (in Chinese).

Tao, T., Shi, Y., Gilbert, K. M., and Liu, X.: Spatiotemporal variations of air pollutants based on ground observation and emission sources over 19 Chinese urban agglomerations during 2015–2019, *Sci. Rep.*, 12, 4293, 720 <https://doi.org/10.1038/s41598-022-08377-9>, 2022.

Tao, Y., Zhang, Z., Ou, W., Guo, J., and Pueppke, S. G.: How does urban form influence PM2.5 concentrations: Insights from 350 different-sized cities in the rapidly urbanizing Yangtze River Delta region of China, 1998–2015, *Cities*, 98, 102581, <https://doi.org/10.1016/j.cities.2019.102581>, 2020.

Wang, C.: New Chains of Space Weather Monitoring Stations in China, *Space Weather*, 8, 725 <https://doi.org/10.1029/2010SW000603>, 2010.



Wang, D., Hu, J., Xu, Y., Lv, D., Xie, X., Kleeman, M., Xing, J., Zhang, H., and Ying, Q.: Source contributions to primary and secondary inorganic particulate matter during a severe wintertime PM2.5 pollution episode in Xi'an, China, *Atmos. Environ.*, 97, 182–194, <https://doi.org/10.1016/j.atmosenv.2014.08.020>, 2014.

Wang, F. T., Zhang, K., Xue, J., Huang, L., Wang, Y. J., Chen, H., Wang, S. Y., Fu, J. S., and Li, L.: Understanding Regional 730 Background Ozone by Multiple Methods: A Case Study in the Shandong Region, China, 2018–2020, *J. Geophys. Res. Atmospheres*, 127, e2022JD036809, <https://doi.org/10.1029/2022JD036809>, 2022a.

Wang, J., Wang, S., and Li, S.: Examining the spatially varying effects of factors on PM2.5 concentrations in Chinese cities using geographically weighted regression modeling, *Environ. Pollut.*, 248, 792–803, <https://doi.org/10.1016/j.envpol.2019.02.081>, 2019.

735 Wang, P., Wang, M., Zhou, M., He, J., Feng, X., Du, X., Wang, Y., and Wang, Y.: The Benefits of the Clean Heating Plan on Air Quality in the Beijing–Tianjin–Hebei Region, *Atmosphere*, 13, 555, <https://doi.org/10.3390/atmos13040555>, 2022b.

Wang, S., Zhou, C., Wang, Z., Feng, K., and Hubacek, K.: The characteristics and drivers of fine particulate matter (PM2.5) distribution in China, *J. Clean. Prod.*, 142, 1800–1809, <https://doi.org/10.1016/j.jclepro.2016.11.104>, 2017.

Wang, Y., Hu, B., Tang, G., Ji, D., Zhang, H., Bai, J., Wang, X., and Wang, Y.: Characteristics of ozone and its precursors in 740 Northern China: A comparative study of three sites, *Atmospheric Res.*, 132–133, 450–459, <https://doi.org/10.1016/j.atmosres.2013.04.005>, 2013.

Wang, Y., Duan, X., Liang, T., Wang, L., and Wang, L.: Analysis of spatio-temporal distribution characteristics and 745 socioeconomic drivers of urban air quality in China, *Chemosphere*, 291, 132799, <https://doi.org/10.1016/j.chemosphere.2021.132799>, 2022c.

Ward-Caviness, C. K. and Cascio, W. E.: A Narrative Review on the Impact of Air Pollution on Heart Failure Risk and Exacerbation, *Can. J. Cardiol.*, 39, 1244–1252, <https://doi.org/10.1016/j.cjca.2023.06.423>, 2023.

Wen, W., Su, Y., Yang, X., Liang, Y., Guo, Y., and Liu, H.: Global economic structure transition boosts PM2.5-related human 750 health impact in Belt and Road Initiative, *Sci. Total Environ.*, 916, 170071, <https://doi.org/10.1016/j.scitotenv.2024.170071>, 2024.

Wilcox, E. M., Thomas, R. M., Praveen, P. S., Pistone, K., Bender, F. A.-M., and Ramanathan, V.: Black carbon solar absorption 755 suppresses turbulence in the atmospheric boundary layer, *Proc. Natl. Acad. Sci.*, 113, 11794–11799, <https://doi.org/10.1073/pnas.1525746113>, 2016.

Xin, Y., Shao, S., Wang, Z., Xu, Z., and Li, H.: COVID-2019 lockdown in Beijing: A rare opportunity to analyze the 760 contribution rate of road traffic to air pollutants, *Sustain. Cities Soc.*, 75, 102989, <https://doi.org/10.1016/j.scs.2021.102989>, 2021.

Yang, J., Shi, B., Zheng, Y., Shi, Y., and Xia, G.: Urban form and air pollution disperse: Key indexes and mitigation strategies, *Sustain. Cities Soc.*, 57, 101955, <https://doi.org/10.1016/j.scs.2019.101955>, 2020.

Yang, W., Yu, C., Yuan, W., Wu, X., Zhang, W., and Wang, X.: High-resolution vehicle emission inventory and emission control 765 policy scenario analysis, a case in the Beijing-Tianjin-Hebei (BTH) region, China, *J. Clean. Prod.*, 203, 530–539, <https://doi.org/10.1016/j.jclepro.2018.08.256>, 2018.

Yang, X., Yang, Y., Xu, S., Karimian, H., Zhao, Y., Jin, L., Xu, Y., and Qi, Y.: Unveiling the air pollution tapestry in China: A comprehensive assessment of spatiotemporal variations through geographically and temporally weighted regression, *Atmospheric Pollut. Res.*, 15, 101987, <https://doi.org/10.1016/j.apr.2023.101987>, 2024.

Yim, S. H. L., Wang, M., Gu, Y., Yang, Y., Dong, G., and Li, Q.: Effect of Urbanization on Ozone and Resultant Health Effects 770 in the Pearl River Delta Region of China, *J. Geophys. Res. Atmospheres*, 124, 11568–11579, <https://doi.org/10.1029/2019JD030562>, 2019.

You, Z., Zhu, Y., Jang, C., Wang, S., Gao, J., Lin, C.-J., Li, M., Zhu, Z., Wei, H., and Yang, W.: Response surface modeling-based source contribution analysis and VOC emission control policy assessment in a typical ozone-polluted urban Shunde,



China, *J. Environ. Sci.*, 51, 294–304, <https://doi.org/10.1016/j.jes.2016.05.034>, 2017.

770 Youn, J., Kim, H., and Lee, J.: Relationships between Thermal Environment and Air Pollution of Seoul's 25 Districts Using Vector Autoregressive Granger Causality, *Sustainability*, 15, 16140, <https://doi.org/10.3390/su152316140>, 2023.

Yu, H., Wang, Y., Yuan, L., Kong, R., Han, S., Han, W., and Li, J.: Longer dust events over Northwest China from 2015 to 2022, *Atmospheric Res.*, 304, 107365, <https://doi.org/10.1016/j.atmosres.2024.107365>, 2024.

Zawacki, M., Baker, K. R., Phillips, S., Davidson, K., and Wolfe, P.: Mobile source contributions to ambient ozone and particulate matter in 2025, *Atmos. Environ.*, 188, 129–141, <https://doi.org/10.1016/j.atmosenv.2018.04.057>, 2018.

775 Zeng, Y., Cao, Y., Qiao, X., Seyler, B. C., and Tang, Y.: Air pollution reduction in China: Recent success but great challenge for the future, *Sci. Total Environ.*, 663, 329–337, <https://doi.org/10.1016/j.scitotenv.2019.01.262>, 2019.

Zhang, A., Xia, C., and Li, W.: Exploring the effects of 3D urban form on urban air quality: Evidence from fifteen megacities in China, *Sustain. Cities Soc.*, 78, 103649, <https://doi.org/10.1016/j.scs.2021.103649>, 2022a.

780 Zhang, W., Zhang, S., Bo, L., Haque, M., and Liu, E.: Does China's Regional Digital Economy Promote the Development of a Green Economy?, *Sustainability*, 15, 1564, <https://doi.org/10.3390/su15021564>, 2023.

Zhang, X., Zhang, M., Cui, Y., and He, Y.: Estimation of Daily Ground-Received Global Solar Radiation Using Air Pollutant Data, *Front. Public Health*, 10, <https://doi.org/10.3389/fpubh.2022.860107>, 2022b.

Zhang, Y., Wang, L., Tang, Z., Zhang, K., and Wang, T.: Spatial effects of urban expansion on air pollution and eco-efficiency: 785 Evidence from multisource remote sensing and statistical data in China, *J. Clean. Prod.*, 367, 132973, <https://doi.org/10.1016/j.jclepro.2022.132973>, 2022c.

Zhang, Y.-L. and Cao, F.: Fine particulate matter (PM2.5) in China at a city level, *Sci. Rep.*, 5, 14884, <https://doi.org/10.1038/srep14884>, 2015.

Zhao, C., Sun, Y., Zhong, Y., Xu, S., Liang, Y., Liu, S., He, X., Zhu, J., Shibamoto, T., and He, M.: Spatio-temporal analysis 790 of urban air pollutants throughout China during 2014–2019, *Air Qual. Atmosphere Health*, 14, 1619–1632, <https://doi.org/10.1007/s11869-021-01043-5>, 2021a.

Zhao, H., Chen, K., Liu, Z., Zhang, Y., Shao, T., and Zhang, H.: Coordinated control of PM2.5 and O₃ is urgently needed in China after implementation of the “Air pollution prevention and control action plan,” *Chemosphere*, 270, 129441, <https://doi.org/10.1016/j.chemosphere.2020.129441>, 2021b.

795 Zhao, S., Yu, Y., Yin, D., He, J., Liu, N., Qu, J., and Xiao, J.: Annual and diurnal variations of gaseous and particulate pollutants in 31 provincial capital cities based on in situ air quality monitoring data from China National Environmental Monitoring Center, *Environ. Int.*, 86, 92–106, <https://doi.org/10.1016/j.envint.2015.11.003>, 2016.

Zhao, X., Zhou, W., Wu, T., and Han, L.: The impacts of urban structure on PM2.5 pollution depend on city size and location, *Environ. Pollut.*, 292, 118302, <https://doi.org/10.1016/j.envpol.2021.118302>, 2022.

800 Zheng, X., Ren, J., Hao, Y., and Xie, S.: Weekend-weekday variations, sources, and secondary transformation potential of volatile organic compounds in urban Zhengzhou, China, *Atmos. Environ.*, 300, 119679, <https://doi.org/10.1016/j.atmosenv.2023.119679>, 2023.

Zhong, S., Qian, Y., Sarangi, C., Zhao, C., Leung, R., Wang, H., Yan, H., Yang, T., and Yang, B.: Urbanization Effect on Winter Haze in the Yangtze River Delta Region of China, *Geophys. Res. Lett.*, 45, 6710–6718, <https://doi.org/10.1029/2018GL077239>, 805 2018.

Zhu, S., Tang, J., Zhou, X., Li, P., Liu, Z., Zhang, C., Zou, Z., Li, T., and Peng, C.: Spatiotemporal analysis of the impact of urban landscape forms on PM_{2.5} in China from 2001 to 2020, *Int. J. Digit. Earth*, 16, 3417–3434, <https://doi.org/10.1080/17538947.2023.2249862>, 2023.